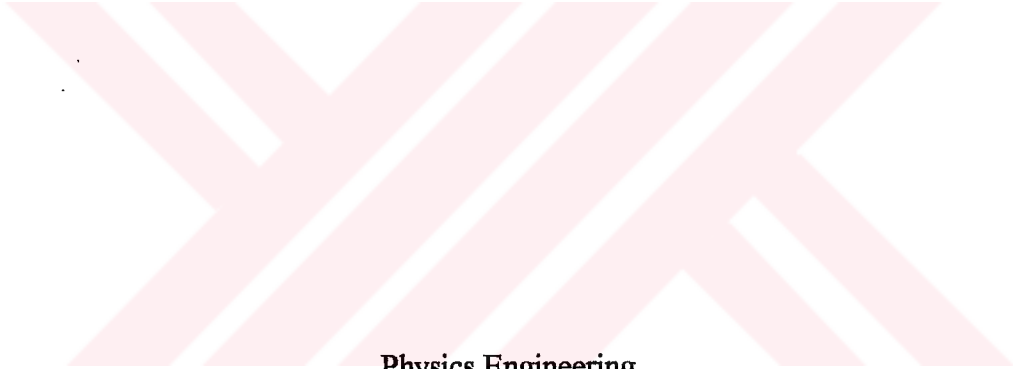# DETERMINATION OF THE KINETIC PARAMETERS OF $CaF_2:Dy$ CRYSTAL BY THERMOLUMINESCENCE METHODS.

A Master's Thesis

Physics Engineering

University of Gaziantep
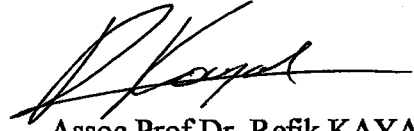
By

Mehmet Yakup HACIİBRAHİMOĞLU

August 1997

Approval of the Graduate School of Natural and Applied Science.

Assoc.Prof.Dr. Ali Rıza TEKİN

Director

I certify that this thesis satisfies all requirements as a thesis for the degree of Master of Science.

Assoc.Prof.Dr. Refik KAYALI
Chairman of the Department

I certify that I have read this thesis and that in my opinion it is fully adequate, in scope and quality, as a thesis for the degree of Master of Science.
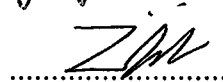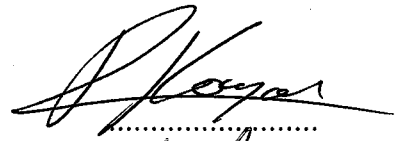
Assist.Prof.Dr.Zihni ÖZTÜRK
Supervisor

Examining Committee in Charge

Assoc.Prof.Dr.Refik KAYALI

Prof.Dr. Mirza BABAYEV

Assist.Prof.Dr.Zihni ÖZTÜRK

ABSTRACT

DETERMINATION OF THE KINETIC PARAMETERS OF CaF_2:Dy CRYSTAL BY THERMOLUMINESCENCE METHODS.

HACIİBRAHİMOĞLU Mehmet Yakup

Ms. Sc. in P.E., University of Gaziantep

Supervisor: Asst.Prof.Dr.Zihni Öztürk

August 1997, 92 Pages

The field of thermoluminescence dosimetry has rapidly expanded during recent years. Especially in environmental and personnel monitoring applications the use of phosphors with low atomic numbers is to be recommended because their responses remain essentially constant through a large spectrum of energies (from low-energy χ-rays to high-energy γ-rays). One of the commercial low-atomic number phosphors is CaF_2:Dy. Up to now no information has been found on the kinetic parameters of glow curve of CaF_2:Dy (TLD-200) dosimeter in literature.

Therefore, this study was undertaken to provide detailed information about the glow curve and kinetic parameters of CaF_2:Dy phosphor. In the course of this study, samples were first irradiated with ^{90}Sr-^{90}Y β-ray source to produce sufficient concentration of defect centers or traps and then thermoluminescence measurements were made to obtain the glow curves. The obtained glow curves were then analyzed by CGCD computer package and other methods such as isothermal decay, peak shape

and initial rise methods. The effects of post-annealing heating rate, dose rate and fading on the glow curve of TLD-200 crystal and its kinetic parameters are widely investigated. The results show that all these processes have great influences on the glow curves and kinetic parameters.

One of the important findings of this work was the determination of the kinetic order of peak VI, which was found to be between 1.55 and 1.6. Other peaks were found to obey the first order kinetic. This study has produced significant results about thermoluminescence properties of TLD-200 (CaF_2:Dy) dosimeter, that were not reported previously.

ÖZET

CaF$_2$:Dy KRİSTALİNİN KİNETİK PARAMETRELERİNİN
TERMOLÜMİNESANS METODLARLA BELİRLENMESİ

HACIİBRAHİMOĞLU Mehmet Yakup

Ms.Sc. F.M. Gaziantep Üniversitesi

Tez Yöneticisi: Y.Doc.Dr.Zihni Öztürk

Ağustos 1997, 92 sayfa

Son yıllarda termolüminesansın kullanım alanı hızlı bir şekilde genişlemiştir. Özellikle çevresel ve kişisel dozimetrik uygulamalarda düşük atom numaralı fosforların kullanılması tercih edilmektedir. Çünkü yüksek değerlikli enerjilere karşı düşük atom numaralı fosforların davranışları önemli derecede sabit kalabilmektedir (düşük enerjili χ-ray'den yüksek enerjili γ-ray'e kadar).Ticari amaçlı düşük atom numaralı fosforlardan biriside TLD-200 (CaF$_2$:Dy) dozimetredir. CaF$_2$:Dy dozimetresinin ısı eğrisinin kinetik parametreleri hakkında literatürde şu ana kadar hiç bir bilgiye rastlanmamıştır.

Bundan dolayı bu tez çalışmasında TLD-200 (CaF$_2$:Dy)dozimetresinin ısı eğrisi ve kinetik parametreleri hakkında detaylı bilgiler elde edilmesine çalışıldı. Çalışmada yeterli yoğunlukta hata ve tuzak merkezleri oluşturmak için numuneler önce ^{90}Sr-^{90}Y β-ışın kaynağı ile radyasyonlandılar, daha sonra ışıldama eğrilerini elde etmek için ısısal ölçümler yapıldı. Elde edilen ışıldama eğrileri CGCD paket proğramı,

sabit ısısal sönümü, pik paylaşım ve ilk yükseliş yöntemi gibi metodlarla analiz edildi. Işınlama sonrası tavlamanın, ısı oranının, doz oranının ve solum zamanının TLD-200 ışıldama eğrisi üzerindeki etkileri detaylı olarak incelendi. Sonuçlar şunu göstermektedir ki; yapılan bütün işlemler ışıldama eğrileri ve kinetik parametreleri üzerinde önemli değişikliklere yol açmaktadır.

Bu çalışmanın önemli sonuçlarından biride tepe 6'nın kinetik mertebesinin 1.55 ile 1.6 arasında olduğunun tespit edilmesidir. Ayrıca diğer tepelerin kinetik mertebelerinin birinci derecede olduğu belirlenmiştir. Bu çalışma TLD-200 dozimetresinin termolüminesans özellikleri hakkında daha önce sunulmamış önemli sonuçlar üretmiştir.

Anahtar Kelimeler : Isı ışıması, $CaF_2:Dy$, TLD-200, Kinetik Parametreler.

ACKNOWLEDGMENT

TABLE OF CONTENTS

LIST OF TABLES

x

LIST OF FIGURES

xiii

xiv

xvi

LIST OF SYMBOLS

A : quantity of absorbance

A : transition coefficient for electrons in the conduction band

A_h: transition coefficient for holes in the valance band

A_r: recombination transition coefficient for electrons in the conduction band

α : absorption coefficient

α : probability of recombination

b : order of kinetic

β : heating rate

C_1: constant

d : lattice constant

D : concentration of thermally stable deep trap

RE: Rare earth element(s)

E : activation energy (trap depth)

E: photon energy

f : electron hole generation rate

I: thermoluminescence intensity

I(E): emission intensity at energy E

$I(E_0)$: emission intensity at the band maximum

k : Boltzmann's constant

λ : wavelength

m : slope

ν : frequency

n : concentration of electrons in the traps

n_c: concentration of electrons in the conduction band

n_h: the concentration holes in the recombination centers

n_v: concentration of holes in the valance band

n_0: initial concentration of trapped electrons

N : the concentration of available electron traps

n_c: concentration of electrons in the conduction band

n_h: the concentration holes in the recombination centers

n_v: concentration of holes in the valance band

n_0: initial concentration of trapped electrons

N : the concentration of available electron traps

N_h: the concentration of available hole centers

p : probability per unit time of the release of an electron from the trap

p_1: probability of stimulation of an electron into the conduction band from deep traps

R: concentration of holes in the recombination centers

δ : high temperature half width

s : frequency factor or pre-exponential factor

t : unit time

T : temperature

T_m: peak temperature

T_0: room temperature

τ : low temperature half width

τ : lifetime of an electron in the trap

CHAPTER 1

Literature Survey

1.1 Introduction

The phenomenon of the thermoluminescence has been well known for a considerable time. In 1663 Robert Boyle reported to the Royal Society on the observation of glow from a diamond when warmed in the dark. A number of other famous scientists such as Henri Becquerel also carried out work on thermoluminescence and in 1904 Marie Curie noted that the thermoluminescent properties of crystals could be restored on exposure to Radium. Further experimental

and theoretical work was carried out by Urbach (1930) in the 1930's; and in 1945 Randall and Wilkins (1945) developed a model which allowed quantitative calculations of thermoluminescence kinetics to be carried out . The application of TL to dosimeter dates from the 1940's when the increase in the numbers of workers exposed to radiation led efforts to seek new types of dosimeter. Daniels (Daniels *et al.*, 1953 [1]) and Cameron (Cameron *et al.*, 1968 [2]) were amongst the pioneers in this field, investigating the properties of LiF as a TL dosimeter. In recent years, interest in TL has continued to increase, not only in dosimetric applications but also as a tool in solid state physics, archaeology, and the earth sciences.

The essential features of the phenomenon of thermoluminescence are as follows. When an insulating crystal is exposed to ionizing radiation, electrons and holes are produced, some of which get trapped in defects in the crystal lattice of the solid . Subsequently, when the temperature is raised high enough to cause the removal of the electrons or holes from their traps they wander around until they recombine at centers giving off light. This phenomenon of emitting light is called thermoluminescence (TL).

Part of the energy absorbed by these insulating materials is emitted during the heating as light in the form of a " *glow curve* " which may present several peaks. The positions, shapes, and intensities of the glow peaks are related to the various parameters of the trapping states responsible for the TL.

The most important parameters to be determined are the trap depth (E), which is the thermal energy required to liberate the trapped electrons or holes, and the frequency factor (s).

Various experimental methods are currently employed for determining trap parameters of the glow peaks. Several of these methods are based on the analysis of glow curves which are reviewed in this thesis, with respect to their advantages and disadvantages.

Thermoluminescent materials include over 2000 natural minerals; a range of inorganic crystals and glasses; pottery and flints used in archeological dating; as well as some organic compounds which luminescence at low temperatures. However, only eight materials are commonly used which have characteristics suitable for use in applied radiation dosimeter. These include four with low effective atomic number Z (similar to that of issue) , namely lithium fluoride (LiF) , lithium borate ($Li_2B_4O_7$), beryllium oxide (BeO) and magnesium borate (MgB_4O_7).There are in addition four non-tissue equivalent materials of higher Z, namely calcium sulfate ($CaSO_4$), aluminum oxide (Al_2O_3), magnesium orthosilicate (Mg_2SiO_4), and Calcium fluoride (CaF_2). Especially , calcium fluoride is doped with various activators which characterize the thermoluminescence properties besides the others. Calcium fluoride exists in nature as fluorite and has been studied in many types and forms as a thermoluminescent dosimeter. The photon sensitivity of CaF_2 (natural) is typically 20 times greater than that of TLD 100. However, the properties depend on the material's origin and a wide range of dose thresholds between 1 and 10 µGy are reported. Optically induced fading can be high in this material (~25 per cent after 4h). however, it has the advantage of a linear response over a wide range of absorbed doses (up to 50 Gy). For synthetic forms of CaF_2 , doping additions of **dysprosium,**

3

thulium and manganese have been used. In Harshaw preparations of the material, these are referred to as TLD 200, TLD 300, and TLD 400, respectively.

Both CaF_2:Dy and CaF_2:Tm **have a complex glow curve structure.** Each glow peak displays a different dose response characteristic and the observation of different LET dependence of the peaks has suggested possible use in mixed field dosimeter. CaF_2:Dy is observed to fade rapidly under most conditions of storage due to the presence of the low temperature peaks. Storage at room temperature in the dark for 24 hours is observed to produce about the 10 percent loss of signal. If the material is kept in diffuse light under similar conditions, fading as high as 30 per cent in a day may result. After this initial high rate of fading, the rate of loss of signal decreases greatly. Therefore, the initial high rate of fading can be allowed for in the calibration of the dosimeter by delaying read-out of a radiation-induced signal for at least a day or by using a post-irradiation anneal at an appropriate low temperature. The sensitivity of CaF_2:Mn is about 5 times that of TLD 100, but only a third that of CaF_2:Dy [3-5]. At low photon energies all types of CaF_2 overrespond by up to a factor of 15 to 20. Despite having a high temperature composite dosimeter peak at ~260 ^{0}C, the fading from this material is initially quite high, corresponding to about 10 per cent in a few hours.

1.2 Literature survey

The dosimeter characteristics of mineral fluorite has been investigated for many decades. The mineral is found to contain a wide variety of impurities of which the rare earth's (RE) are the most important from the stand point of fluorescence. The study of RE ions (Gd, Dy, Er, Tm, Tb, Yttrium, Ti, and Mn) in fluorite host lattice gained momentum when the need to develop materials for lasers and optical frequency converters, and they also provided an important avenue for spectroscopic and solid state studies, especially in dosimetric field.

Natural and Mn doped calcium fluoride were among the first materials used for the measurement of ionizing radiation dose through phenomenon of thermoluminescence (Becker, 1973[6]; Horowitz, 1984[7]; McKeever, 1985[8]). Rare-earth impurity ions and the associated defect centers, acting as a charge carrier traps, are crucial to the observance of strong thermoluminescence in natural fluorite (Arkhangel'skaya, 1964[9]; Merz and Porshon, 1967[10]; Sunta, 1984[11]). This is also evidenced by the study of RE ion doped synthetic calcium fluoride. The most successful dopiness in this respect are **dysprosium (Dy)** and **thulium (Tm)**. Manganese (Mn) doped calcium fluoride is also a widely used as radiation dosimeter material.

Many investigations have been done to understand the structure and thermoluminescence of CaF_2:Tm, CaF_2:Mn and CaF_2:Dy and other CaF_2 based dosimeters. CaF_2:Tm has several peaks in its glow curve. The two most prominent occur at temperature of about 150 ^{0}C and 240 ^{0}C. These two peaks are used for radiation dosimeter. The emission spectrum, annealing and fading properties of

5

CaF$_2$:Tm have been studied by many researchers (Driscoll *et al.*, 1986[12]; Furetta and Lee, 1983[13])

CaF$_2$:Mn has long been in use for radiation dosimeter (Horowitz, 1984 [7]). Its dosimetric characteristics are well described in Horowitz (1984, p.141[7]). The Glow curve has generally been described as containing a single peak at about 250 ^{0}C, there are other low peaks which decayed during the 24 h post-irradiation storage. At optimum concentration CaF$_2$:Mn is the most sensitive CaF$_2$ based TL material, about 10 times as sensitive as the others. The TL response of CaF$_2$:Mn has also been investigated below temperature (Alonso *et al.*, 1980[14]; Jain & Jahan, 1985 a, b, c [15-17]). Kinetic parameters of this material have also been obtained by several researchers.

CaF$_2$:Dy has 5 peaks, irradiated to 0.3 Gy ^{60}Co γ-rays at room temperature, recorded 24 h after irradiation (Pradhan & Rassow, 1987[18]). Because of dominant low temperature peaks, there is a considerable amount of fading of total TL output if the dosimeter is stored at room temperature. The luminescence spectrum (444, 474 and 568 nm) has been identified as due to the Dy^{3+} ion, and to remain the same at all doses (Horowitz, 1984 [7]).

CaF$_2$:Dy (TLD-200) detectors, with suitable filters are used, for dose determination due to low energy photons (< 100 keV), charged particles and muons around a high energy proton accelerator. Its response to β-radiation of different maximum energies has also been determined (Driscoll *et al.*, 1984[19]).

Some other activators for CaF$_2$ have also been tested, among them erbium and terbium. Apparently they offer no substantial advantages. A supposedly " *pure*" synthetic CaF$_2$ sample exhibits peaks at 60 and 360 ^{0}C, the ratio between both

changing during fading, for example, by a factor of two during five days at 10 ^{0}C. It is, in principle, possible to use this ratio as an indicator of time of exposure. Compared to the vast literature on LiF:Mg:Ti (TLD-100), relatively little work has been done on CaF$_2$:Dy (TLD-200) and CaF$_2$:Tm (TLD-300) crystals. Our literature survey indicates that very few studies on the thermoluminescence properties and defect structure of CaF$_2$:Dy dosimeter have been reported, however no work has been found on the kinetic analysis of the glow peaks of CaF$_2$:Dy dosimeter. Therefore, it was decided to take this study on the CaF$_2$:Dy crystal and to carry out experiments to valuate the kinetic parameters of the glow peaks, especially the peak six, which seems to have an interesting structure.

CHAPTER 2

THEORY

2.1 Theory

One of the prime objectives of a thermoluminescence experiment is to extract data from an experimental glow curve, or a series of glow-parameters associated with the charge transfer process in the material under study. These parameters include the trap depths (E), the frequency factor (s),kinetic order (b) or (l), etc. Of course, arriving at values for these parameters does not necessarily mean that we fully understand them, or that we are knowledgeable about the defect model with which they are associated. Nevertheless, calculations of this sort are an important step in arriving at an acceptable level of understanding of the underlying processes and a great deal of effort has been directed towards the development of a reliable method of analysis.

The most popular procedure begins by selecting the rate equations appropriate to a particular model and continues by introducing simplifying assumptions into these equations in order to arrive at an analytical expression which describes the variation in thermoluminescence intensity with temperature, in terms of the desired parameters. From these equations even simpler expressions are produced which relate the parameters directly to the data. However, this procedure firstly requires an assumption as to which model is used to describe the thermoluminescence production; and secondly , by introducing further assumptions into the chosen rate equations, additional restrictions are being brought into play which inevitably limit the generality, and possibly the validity of the results obtained. Invariably, the model which is most often chosen for analysis is the simple two-level model, sometimes with the addition of a third level (thermally disconnected traps). However, more often than not, no tests are carried out to (a) check the validity of the simple model, and (b) confirm that the approximations introduced are indeed applicable. Some of these approximations place severe restrictions on the kinetics of thermoluminescence emission. Fortunately, this is becoming recognized as an important factor in thermoluminescence analysis and many experimenters are making great efforts to try to be certain about the order of kinetics appropriate to their case. Nevertheless, other approximations (such as the constancy of the electron distribution in the conduction band) remain unverified, and the chosen energy level model stays unconfirmed. The reason for this lack of verification is quite straightforward-it is experimentally very difficult to do. Progress on this front has recently been made by the Montpellier(France) group who, by simultaneous measurement of thermally stimulated conductivity and thermoluminescence, have developed an experimental

9

means of testing certain aspects of the two-level model (Fillard *et al.*, 1977[20], 1978[21]; Gasiot and Fillard, 1977 [22]). Additionally, theoretical exercises, such as those of Kelly *et al.* (1971 [23]), Shenker&Chen(1972) [24] and Kivits and colleagues (Hagebeuk&Kivits, 1976 [25]; Kivits&Hagebeuk,1977 [26]; Kivits, 1978 [27]), help to develop an understanding of the effects of the various assumptions on the analyses. However, all of these works deal with simultaneous measurements of thermally stimulated conductivity and thermoluminescence, and this is experimentally difficult to perform. Thus with measurements of thermoluminescence alone (the vast majority) one can not carry out these checks with the final results are often doubtful, or difficult to interpret.

However, the prospect of using thermoluminescence alone to arrive at values for the various trapping parameters is not quite as gloomy as this discussion implies so far. Recent analyses and arguments indicate that certain methods of analyses can still be successfully applied despite the introduction of approximate solutions of different rate equations (appropriate to particular model) suggest that the actual model may also not be so important, in that trap depths and frequency factors may still be calculated. The problem then becomes one of interpreting the meaning of the results obtained. Although acceptable values of the parameters may be arrived at and these values may then be used to predict successfully the shape and behavior of the thermoluminescence glow-curve, this unfortunately does not allow the experimenter to be definite about any model[8].

10

2.1.1 Simple Models for Thermoluminescence

The simplest model for TL consists of a single type of electron defect level and a single type of hole defect level in the forbidden gap, as depicted in Figure 1. It must be required to remember in here that two energy level band model is the minimum number needed in order to describe the thermoluminescence mechanism. But, the band model of an actual specimen may be much more complex than this simple model. However, this simple model is enough to explain the fundamental features of TL production. If the electron level is relatively shallow in the forbidden gap, the hole
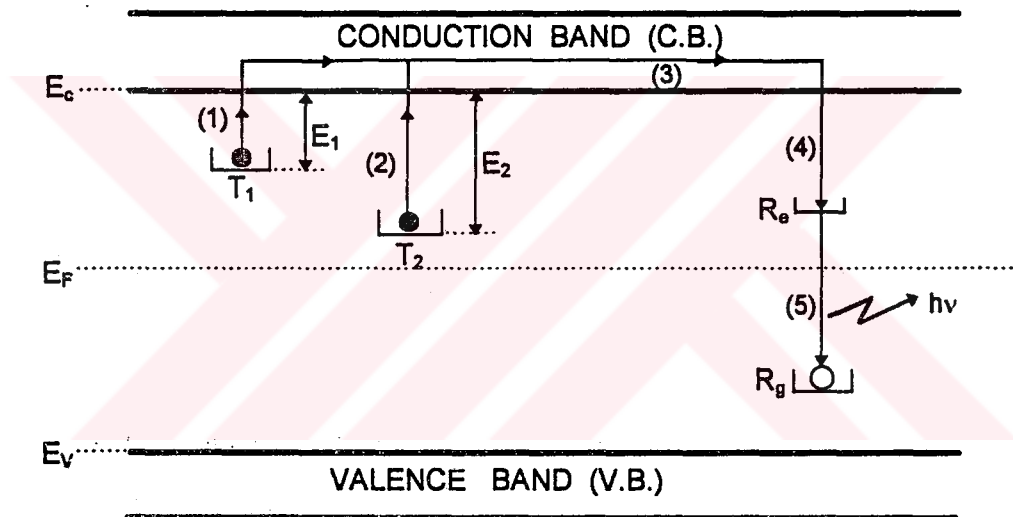
Figure 1 Simple band model for TL emission. T_1 and T_2 are electron traps, R_e and R_g are the excited and ground state of a recombination (luminescent) center, E_1 and E_2 are the energy differences between the band edge of the conduction band and electron trap T_1 and T_2, respectively. Allowed transitions: (1) and (2) thermal release, (3) migration, (4) non-radiative recombination, (5) radiative recombination.

center is thermally stable during the heating, while electrons are thermally released and move the conduction band. Eventually they recombine with the hole centers to produce TL. The shallower level is called "trap" and the other one "recombination center" or "luminescent center".

The probability p per unit time of the release of an electron from the trap to the conduction band can be calculated by the Arrhenius equation:

$$p = \tau_e^{-1} = s \exp(-\frac{E}{kT}) \qquad (1)$$

where τ_e is defined as the lifetime of an electron in the trap, E (activation energy) is the vertical energy separation between the trap and the conduction band which is frequently called as the trap depth (eV), s (sec^{-1}) is the attempt to escape frequency from the trap which is frequently called as " frequency factor " or "pre-exponential factor", k is the Boltzmann's constant and T is the temperature.

As can be understood from Arhenius equation, if the trap depth E is greater than kT_0, where T_0 is the irradiation temperature, then any electron which becomes trapped will remain so for a long period of time. If the temperature of the specimen is raised above T_0 such that E≤kT, this will increase the probability p and the electron will now be released from the trap into the conduction band. Therefore, the recombination rate increases at first because more trapped charge carriers are released per second. As the electron traps are progressively emptied, then, after reaching a maximum the rate of recombination decreases and thus the TL intensity decreases accordingly. Thus, it can be said that TL is highly depend on the trap depth E (eV) and frequency factor s (sec^{-1}) and the concentration of the traps.

2.1.2 Trap Filling Process

During the irradiation, the trap filling process is described by Chen,

McKeever and Durrani (1981)[28] by the following four equations:

$$\frac{dn_c}{dt} = f - n_c A_r n_h - n_c (N - n) A \tag{2}$$

$$\frac{dn}{dt} = n_c (N - n) A \tag{3}$$

$$\frac{dn_v}{dt} = f - n_v (N_h - n_h) A_h \tag{4}$$

$$\frac{dn_h}{dt} = n_v (N_h - n_h) A_h - n_c n_h A_r \tag{5}$$

where n_c is the concentration of electrons in the conduction band (per unit volume, m^{-3}),

n_v is the concentration of holes in the valance band, n is the concentration of electrons in

traps, N is the concentration of available electron traps (of depth E below the conduction

band), n_h is the concentration of holes in the recombination centers, N_h is the concentration

of available hole centers, A is the transition coefficient for electrons in the conduction band

becoming trapped (volume/until time $m^3 sec^{-1}$), A_h is the transition coefficient for holes in

the valance band becoming trapped in the hole centers, A_r is recombination transition

13

coefficient for electrons in the conduction band with holes in centers and f is the electron hole generation rate.

2.1.3 Trap Emptying Process

Assuming a single electron trap and a single hole center, the rate equations describing the flow of charge between the various energy levels and bands during trap emptying have been described by Adirovitch (1956)[29], Haering and Adams (1960)[30], and Halperin and Braner (1960)[31] and given in following form:

$$\frac{dn_c}{dt} = ns \exp[-\frac{E}{kT}] - n_c(N-n)A - n_c n_h A_r \qquad (6)$$

$$\frac{dn}{dt} = n_c(N-n)A - ns \exp[-\frac{E}{kT}] \qquad (7)$$

$$I_{TL} = -\frac{dn_h}{dt} = n_c n_h A_r \qquad (8)$$

where I_{TL} is the TL intensity (photons/sec). According to equation (8), I_{TL} is equal to the rate of recombination, which is proportional to the number of recombination centers and the number of free electrons.

Unfortunately, there is no general analytical solution of these equations (6), (7) and (8), however, an approximate solution can be achieved by making some simplifying assumptions. Alternatively, numerical solutions can be found for a given set of the

14

parameters E, s, Ar, A, N, Nc, n_c , n and n_h [32-34]. These numerical solutions are quite useful for studying the dependence of the TL curve on the various parameters.

In order to obtain an analytical solution of equations (6), (7) and (8), usually, the following two assumptions are employed

$$n_c << n, \qquad \frac{dn_c}{dt} << \frac{dn}{dt}.$$ (9)

It was also assumed that the charge neutrality condition becomes

$$n_c + n = n_h$$ (10)

which for $n_c \approx 0$ means $n = n_h$ and $dn/dt \approx dn_h/dt$. Since $dn_c/dt \approx 0$ one gets from equations (6), (7) and (8);

$$I_{TL} = -\frac{dn_h}{dt} = \frac{ns \exp(-\frac{E}{kT})}{1 + \frac{(N-n)A}{nA_r}}$$ (11)

Although Eq.(11) is simpler than Eqs.(6), (7), (8), it cannot be solved analytically without additional simplifying assumptions. When retrapping can be neglected, i.e., (N-n)A<<nA_r, one gets (by substituting n_h=n) the famous first-order kinetics (Randal & Wilkins 1945a,b)

$$I_{TL} = -\frac{dn}{dt} = ns \exp(-\frac{E}{kT})$$ (12)

15

If the coefficients for retrapping and recombination are equal i.e., $A = A_r$ and the assumptions $n \ll N$ and $n = n_h$, the Eq.(11) yields the second-order kinetics

$$I = -\frac{dn}{dt} = n^2 s' \exp(-\frac{E}{kT})$$ (13)

where $s' = sA/NA_r$, and the power of n in eqs.(12) and (13) indicates the order of kinetics. However, when the simplifying assumptions do not hold, the TL peak will fit neither the first- nor the second-order equation,

$$I = -\frac{dn}{dt} = n^b s'' \exp(-\frac{E}{kT})$$ (14)

where b is the kinetic order, s'' is frequency foctor. Equation (14) is called the general-order kinetics which was first proposed by May and Patridge (1964)[35]. Eqs. (12) and (13) are known as the special cases of the general order kinetics eq.(14) with b=1 and b=2 respectively.

The solution of Eq.11, assuming a linear heating rate program b (^{0}C/sec), gives the famous first-order equation of Randal & Wilkins,

$$(T) = n_0 s \exp(-\frac{E}{kT}) \exp(-\frac{s}{\beta} \int_{T_0}^{T} \exp(-\frac{E}{kT'})dT')$$ (15)

The solution of Eq.(13) gives the second-order equation of Garlick & Gibson (1948) [36] as

$$(T) = n_0^2 s' \exp(-\frac{E}{kT})[1 + \frac{n_0 s'}{\beta} \int_{T_0}^{T} \exp(-\frac{E}{kT'})dT']^{-2}$$ (16)

16

and the solution of eq.(14) for b $\neq$ 1 is

$$(T) = n_0 s'' \exp(-\frac{E}{kT})[1+\frac{(b-1)s''}{\beta}\int_{T_0}^{T}\exp(-\frac{E}{kT'})dT']^{\frac{b}{b-1}} \quad (17)$$

where T_0 and n_0 are the initial temperature and initial concentration of trapped electrons, respectively, and $s'=s/N$, $s''=s'n_0^{(b-1)}$. The values of b lies in general between 1 and 2 but, in principle, values of b outside this range are also possible.

2.2.1 Methods For Determining The Trapping Parameters

There are various methods for evaluating the trapping parameters namely as activation energies E (trap depth), frequency factor s (attempt-to-escape frequency or pre-exponential factor), kinetic order b, the number of trapped electron concentrations n_0. Some of them are listed below:

(1) Initial rise method

(2) Peak shape method

(3) Isothermal decay method

(4) Computer curve fitting method

2.2.2 The Computation of s

The second exponential terms in Eqs.(15), (16) and (17) become more important at high temperatures than first exponential terms. Thus a maximum T_m temperature is always observed at a certain temperature in glow curves. Thus at the maximum intensity I_m, by equating the derivative of I with respect to T to zero (dI/dT=0) when $T=T_m$ or the derivative of ln(I) (dln(I)/dT=1/I(dI/dt)=0 at $T=T_m$), the Equation (15) yields

$$s = \frac{\beta E}{kT_m^2} \exp(\frac{E}{kT_m}) \qquad (18)$$

Similarly, from Eq.(17) for the general order kinetics, one gets

$$s = \frac{\beta E}{kT_m^2} [\exp(-\frac{E}{kT_m})(1+(b-1)\frac{2kT_m}{E})]^{-1} \qquad (19)$$

Once the value of E was determined, the frequency factor s can be obtained from the equation (18) for a first order case. However, for other kinetics, the values of b are required to be known previously. Therefore, the value of b must be obtained by other methods previously. Then using the equation (19), one can obtain the value of s (frequency factor, s^{-1}).

18

2.2.3 The Computation of E

2.2.3.1 Initial Rise Method

At first, the trap depths of the glow peaks were obtained by the initial-rise method (Garlick & Gibson 1948)[36] for the glow peak intensity I(T). In the region, where $T \ll T_m$ (up to 10 to 15 % of I_m) all the factors other than exp(-E/kT) in the Eqs. (15),(16) and (17) do not show an appreciable variation with T and therefore the intensity is proportional to exp(-E/kT) according to the expression

$$I \; \alpha \; \exp(-\frac{E}{kT}) \qquad\qquad (20)$$

for either type of kinetics. Thus, plotting ln(I) as a function of 1/T produces a straight line with a slope equal to -E/k from which the value of E can be found.

When s depends on the temperature with $s = s_0 T^a$, a correction factor comes to the activation energy with $E = E_{ir} - akT_m$, where E is the true activation energy and E_{ir} is the value measured by the initial rise method and the value of a usually lies from -2 to +2. If ignoring this correction factor, the true activation energy may distort from the real value by 5 to 10 %.

The initial rise method does not give any information on b. Actually the low temperature side of the peak is not very sensitive to the kinetic order b.

19

2.2.3.2 Peak Shape Methods

This method based on the shape of the peak utilizes just two or three points

from the glow-curve. Usually, these are the maximum of the peak T_m and either or

both, the low and high-temperature half-heights at T_1 and T_2 (see Figure 2).
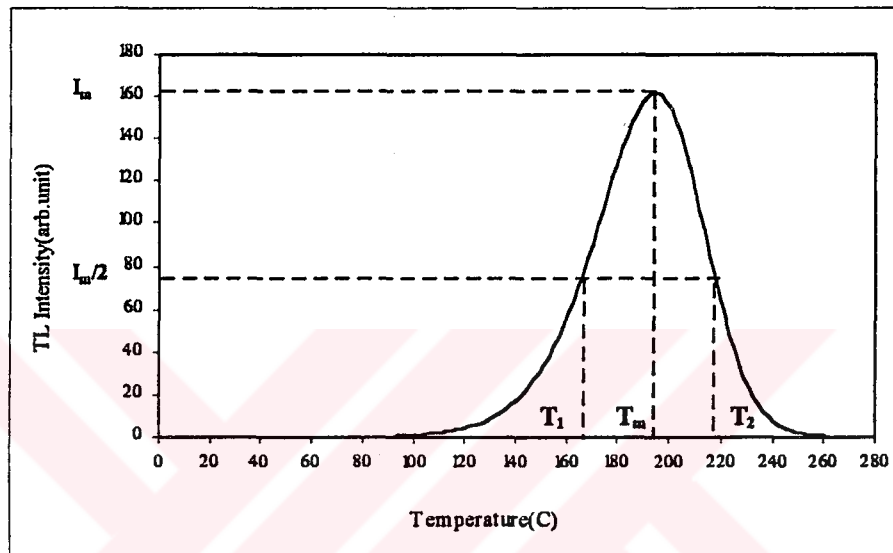
Figure 2 : A typical glow curve shape. $\tau=T_m-T_1$, $\delta=T_2-T_m$, $\omega=T_2-T_1$. The ordinate

shows TL intensity.

The peak shape method used in this thesis were those of Grossweiner

(1953)[37], Lushchik (1956)[38], Halperin & Braner (1960)[39] and Chen (1969a,b)

[40].

Grossweiner[37] has suggested the following approximate equation for finding

the activation energy using the value of t

$$E = a\frac{kT_1T_m}{\tau} \tag{23}$$

where $\tau = T_m - T_1$, a $= 1.41$ or 1.68 for first and second-order kinetics respectively.

Lushichik[38] obtained two different expression for first and second order kinetics based on the measurement of $\delta = T_2 - T_m$. For first and second order kinetics the Eq.(23) was modified by Chen (1969b)[40] as

$$E = 0.976 \frac{kT_m^2}{\delta} \quad (b = 1)$$

$$E = 1.706 \frac{kT_m^2}{\delta} \quad (b = 2) \tag{24}$$

Halperin & Braner (1960)[39] suggested a method based on the measurement of T_1 and T_m for the both first and second order cases. Considering the τ and the correction by Chen (1969b)[40], the expression were as follows:

$$E = 1.52 \frac{kT_m^2}{\tau} - 3.16 kT_m \quad (b = 1)$$

$$E = 1.813 \frac{kT_m^2}{\tau} - 4.0 kT_m \quad (b = 2) \tag{25}$$

In addition to these formulas, Chen (1969a,b) also analyzed these methods to their fullest extent. Chen (1969a) gives three equations each for first and second order peaks, uses total-half width $\omega = T_2 - T_1$, low-temperature half-width $\tau = T_m - T_1$ and high-temperature half-width $\delta = T_2 - T_m$. A general formula for E was given as:

$$E_a = c_a \frac{kT_m^2}{a} - b_a (2kT_m) \tag{26}$$

where a stands for δ, τ or ω and the values of coefficients c_a and b_a for the three

21

methods are:

$$c_\tau = 1.510 + 3.0(\mu_g - 0.42)$$

$$c_\delta = 0.976 + 7.3(\mu_g - 0.42)$$

$$c_\omega = 2.52 + 10.2(\mu_g - 0.42)$$

$$b_\tau = 1.580 + 4.2(\mu_g - 0.42)$$ \hspace{2cm} (27)

$$b_\delta = 0$$

$$b_\omega = 1$$

If the temperature dependence of the frequency factor of the type $s = s_0 T^a$ is suspected, then a term $a/2$ must be added to the constants b_a. Chen has also discussed the determination of the geometrical factor $\mu_g = \delta/\omega$ for different values of b. The resultant variation of μ_g with β has been used to determine the value of kinetic order b from the experimental glow curve.

2.2.3.3 Isothermal Decay Method

Another method for determining trapping parameters is the isothermal decay method, which is not exactly a TL method. It deals with phosphorescence rather than TL. According to this method, if TL material is held at a constant temperature, the luminescence emission can be recorded as a function of time while TL material is held at a constant temperature, rather than being heated up. For first order kinetic, by solving Eq. (16) for constant T, the decay in intensity is given by

$$I(t) = n\, s\, \exp\left(-\frac{E}{kT}\right) \times \exp\left[-s\, t\, \exp\left(-\frac{E}{kT}\right)\right]$$ \hspace{1cm} (28)

A plot of ln(I) against time is linear and the slope m is given by

$$m = s\exp(-\frac{E}{kT})$$
(29)

If the experiment is carried out at two different constant temperatures T_1 and T_2, two different slopes, m_1 and m_2, are obtained and from these two slopes one obtains

$$\ln(\frac{m_1}{m_2}) = (-\frac{E}{k})(\frac{1}{T_1} - \frac{1}{T_2})$$
(30)

2.2.3.4 Computerized Curve Fitting Method

The trapping parameters E, s, n_0, b for the individual peaks can be calculated by a method of computerized curve fitting. Initially, the fitting method starts from the general-order kinetic expression for each peak then tries to fit with first-order kinetics, The expressions for these two equations are:

$$I(T) = n_0 s \exp(-\frac{E_a}{kT}) \times \exp[-\frac{s}{\beta} \frac{kT^2}{E_a} \exp(-\frac{E_a}{kT}) \times (0.992 - 1.620\frac{kT}{E_a})] \tag{31}$$

and

$$I(T) = n_0 s \exp(-\frac{E_a}{kT}) \times [1 + \frac{(b-1)s}{\beta} \frac{kT^2}{E_a} \exp(-\frac{E_a}{kT})(0.992 - 1.620\frac{kT}{E_a})]^{\frac{b}{1-b}} \tag{32}$$

The symbols have the usual meaning. The integrals in these formulas are calculated by approximating, and used to get best fits between experimental glow curve and theoretical one.

For each choice of $I_i(T)$, due to the experimental apparatus the complete glow peak is given by[41-43]

$$G(T) = \sum^{2} I_i(T) + A + B \exp CT \tag{33}$$

Where $G(T)$ is the fitted total glow curve, A allows for the electronic noise contribution to the total background and B and C are related to the planchet and dosimeter infrared contribution to the background. However, in this study, A and B

factors are not used. Because they are not basically essential due to the $I_i(T)$.Hence the last equation became

$$G(T) = \sum I_i^2(T) \qquad (34)$$

Starting from the above equation and using CGCD, Chi-squared method(the least square method) and FOM(Figure of Merit) are applied to check the deviation from the average value or to determine the standard deviation of the calculated values. A difficulty in comparing the outcomes of the measurement arises due to the fact that 'true" parameter values are not known. In order to compare the results the standard deviation of the calculated values should be determined. However, it should be born in mind that the averaged value may deviate from 'true"value. That's why, it is generally considered that the FOM, and Chi-squared methods control the calculations.

The ,Chi-squared method, χ^2 function has been minimized, being

$$\chi^2 = \sum_T \frac{[N(T) - G(T)]^2}{G(T)} \qquad (35)$$

where N(T) is the experimental value of thermoluminescence light at temperature T, and G(T) is the expected value of N(T). The experimental data counts N(T) are distributed as a Poisson variable with mean value $\mu \geq 10$. Therefore, the Poisson variable can be approximated by a Gaussian variable and the Chi-squared method is applicable.

Since N(T) is a Poisson variable, the estimated variable can be expressed by $\sigma^2(T)=G(T)$. In order to get a graphic representation of the agreement between experimental and fitted glow peaks, the computer program plots the function χ, which is a normal variable with an expected value 0 and $\sigma = 1$. In equation (35), the difference N(T) - G(T) is the residuals and $\sigma(T)$ is the expected residuals. The squares are to remove the signs. The value of, Chi-square, χ^2 highly depends on the estimated error in data points. Before drawing any conclusion about model one should be sure that error estimation is right.

A better measure of goodness-of-fit is to simplify sum of all the residuals and express the value as a percentage of the integrated intensity

$$\text{Figure-of-Merit,} \qquad FOM = \sum \frac{(Y_i - T_i)}{A} = \sum \frac{\Delta Y_i}{A} \qquad (36)$$

$$A = \int_{Range} \text{Fitted function}$$

For a spectrum with a background

$$FOM = \sum_p \frac{\Delta Y_i}{A_p} + \sum_b \frac{\Delta Y_i}{A_b} \qquad (37)$$

From experiences,[44] it is said for all types of peaks that :

$$\text{good fit} \qquad \Leftarrow \qquad 0.0\,\% < FOM < 2.5\,\% \qquad (38)$$

$$\text{small flow} \qquad \Leftarrow \qquad 2.5\,\% < FOM < 3.5\,\% \qquad (39)$$

26

$$\text{bad fit} \quad \Leftarrow \quad \text{FOM} > 3.5\,\% \qquad (40)$$

However FOM may be a poor measurement for spectra with low backgrounds. In the case of a low background A_b is very small and so the background term in upper equation can give a very large contribution to the FOM (artificially increasing FOM). Also small flows in the tails of peaks can give large values of FOM.

Now there are FOM and IFOM. IFOM (improved figure-of-Merit)[45] is

$$\text{IFOM} = \frac{n_p}{(n_p + n_b)} \sum_n \frac{\Delta Y_i}{A_p} \qquad (41)$$

where n_p is the channels for the peak and $n_p + n_b$ is the total number of channels in the fit. It appears that the upper equation is true when we include background terms. For glow spectra, which are insignificantly small and one can remove these background terms (So in this thesis, there is no background terms, hence the glow peaks can be analyzed only with FOM) .

In this case upper equations become

$$\text{FOM} = \sum_p \frac{\Delta Y_i}{A_p} \qquad (42)$$

$$\text{IFOM} = \sum_p \frac{\Delta Y_i}{A_p} \qquad (43)$$

Which means that FOM and IFOM are the same. The program saves Chi-squared value and FOM value at the same time to the file which leads somebody to

get more information about fitting and all parameters.   The program, (CGCD),

is capable ofsimultaneously deconvoluting as many as nine glow peaks that have ,

optional, 30 parameters for any fitting curve.

CHAPTER 3

EXPERIMENTAL PROCEDURE

3.1 Introduction

The experimental procedure, equipment and materials utilized in this work are described below.

3.1.1 Material

The samples, used in this work are CaF_2:Dy (TLD-200) single crystalline chips obtained from Harshaw/Filtrol Chemical Company which produces CaF_2:Dy that has a gamma ray response at [60]Cobalt energies 30 times greater than LiF, and several times that of CaF_2:Mn. TLD-200 is probably the best TLD material for short term environmental applications. Features include:

1- Extreme sensitivity; capable of measuring one day of natural background radiation (~0.25 mR)± 25 %.

2- Solid dosimeters

3- 100 % calcium Fluoride

4- Mechanically rugged

5- Optical transparent

6- Sample-to-sample uniformity

7- Reusable

8- Wide range of exposures < 1 mR to > 10^6 R

9- Energy dependence below several hundred keV; can provide two point energy spectrum approximations when used with Harshaw LiF high sensitivity ribbons

10- Long term response retention

11- Approximates the ideal "point radiation detector".

3.1.2 Standard geometry of this TLD material

Dosimeters have the dimensions of 3.1 × 3.1 × 0.89 mm (0.125 × 0.125 × 0.035") and weigh approximately 16 mg. The concentration of Dy impurity in these specimens has been found by different workers to vary from 150 to 250 ppm [46].

3.2 Heat Treatment

The experiments were carried out to observe the effect of the pre- and post-irradiation heat treatment on the glow curves. The annealing procedures were done at different temperatures with a microprocessor controlled Nuve FN 501 type electrical oven for different intervals ranging between 1 min. to 24 hours. The temperature is measured with a Chromel-Alumel thermocouple placed in close proximity to the samples. Temperature of the electrical oven was continuously monitored during the annealing period. The temperature sensitivity of the oven was estimated to ± 1 ^{0}C for the whole temperature range employed from room temperature to 350 ^{0}C.

The standard annealing process was done for all samples to remove any trapped defect centers which can interfere with subsequent emission and absorption measurement prior to every irradiation. In this case, the samples were held at 400 ^{0}C for 10 minutes in a microprocessor controlled Nuve MF 120 type electrical oven. This oven is used for the high temperature annealing between 400 ^{0}C and 1200 ^{0}C with a relatively low sensitivity such as ± 10 ^{0}C. The samples were quenched to room temperature by a cooling rate at approximately 10 ^{0}C per second following every annealing process by withdrawing the samples from the oven onto a aluminum disk.

3.3 Radiation Source and Irradiation Procedure

The samples were irradiated at room temperature immediately after quenching. All irradiation were carried out with ^{90}Sr-^{90}Y β-source. The activity of β-source is about 100 mCi. It is calibrated by manufacturer on March, 10 1994. The recommended working life-

time is about 15 years. Strontium-90 emit high energy beta particles from their daughter products (^{90}Sr β-0.546 MeV together with ^{90}Y β-2.27 MeV). Beta radiation is absorbed by air, so its intensity declines with distance much more rapidly than inverse square law calculations would indicate. The maximum range of Y-90 beta particles in air is approximately 9 meter. The typical strength of a 100 mCi Sr-90 β-source installed in a 9010 Optical Dating System is 2.64 Gy/minute= 0.0428 Gy/Sec for fine grains on aluminum, or 2.2 Gy/min= 0.055 Gy/sec for 100 m quartz on stainless still. The irradiation equipment is an additional part of the 9010 Optical Dating System which is purchased from Little More Scientific Engineering, UK [47]. The irradiation source equipment interfaced to a PC computer using a serial RS-222 port. During the investigation of pre-irradiation effects on the TLD-200, the irradiation duration were adjusted to 5 minutes for TL spectra .

3.4 TL Analyzer and Measurements

The glow curve measurements were made using a Harshaw TLD System 3500 Manual TL Reader [46]. It economically provides high reliability. The technical architecture of the system includes both the Reader and a DOS-based IBM-compatible computer connected through a standard RS-222 serial communication port to control the 3500 Reader. The basic block diagram of reader is shown in figure 3. All functions are divided between the reader and the specialized TLDShell software that runs on the PC. All data storage, instrument control, and operator inputs are performed on the PC.

Signal acquisition and conditioning are performed in the reader. In this way, each glow curve can be analyzed using a best-fit computer program based on a Marquardt algorithm minimization procedure, associated to first-order and general-order kinetic expressions. The program resolves the individual peaks present in the curve, giving the best values for the different peak parameters.

The instrument includes a sample change drawer for inserting and removing the TLD elements. The reader uses contact heating with a closed
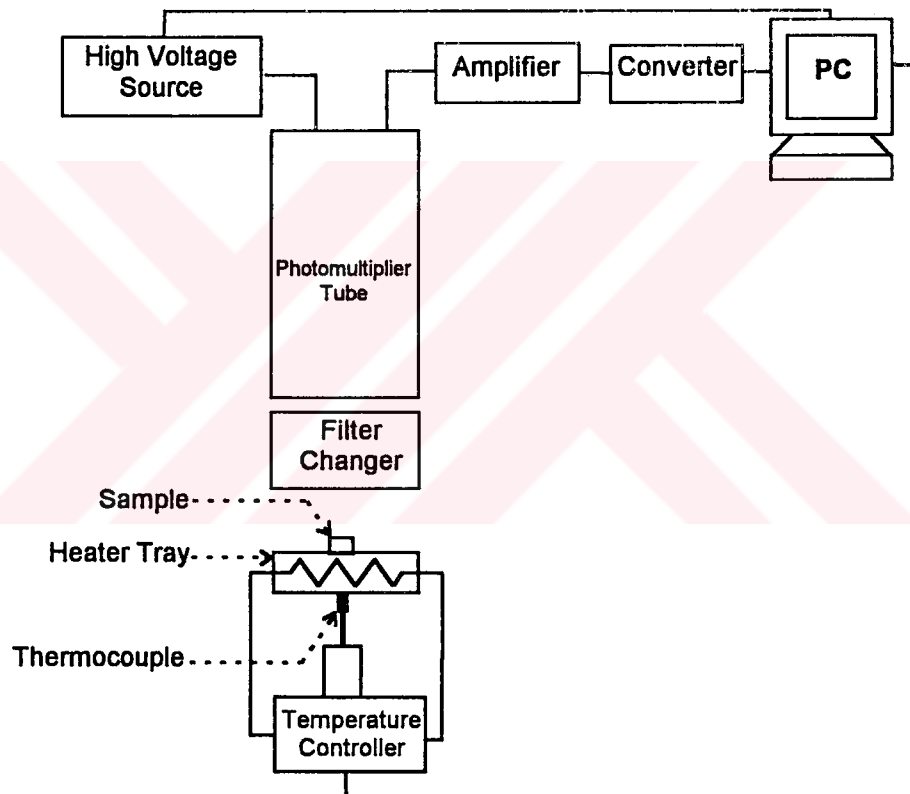
Figure 3. Basic block diagram of TL reader.

loop feedback system that produces adjustable linearly ramped temperatures from 1^0C to 50^0C per second accurate to within ± 1 ^{0}C to 400 ^{0}C in the standard reader. The Time Temperature Profile (TTP) is defined in three segments: Preheat, Acquire, and Anneal, each with independent times (Pre-read anneal: adjustable 0 to 1000 sec, Linear ramp:

adjustable from 1 ^{0} to 50 ^{0} per second, Post-read anneal: 0 to 1000 sec) and temperature (Pre-read anneal: room temperature to 200 ^{0}C, Post-read anneal up to 400 ^{0}C). The typical time temperature profile is shown in figure 4.

To improve the accuracy of low-exposure readings and to extend planchet life, the 3500 provides for nitrogen to flow around the planchet. By eliminating oxygen in the planchet area, the nitrogen flow eliminates the unwanted oxygen-induced TL signal. N_2 is also routed through the photo-multiplier tube (PMT) chamber to eliminate moisture caused by condensation. Due to the high cost of Ni consumption, during the measurement Ni was not used.

ANNEAL TEMP.

MAX TEMP.

50 ^{0}C/S

MAX TEMP. RAMP RATE

TEMP. (^{0}C)

PREHEAT TEMP.

TEMPERATURE RAMP RATE

30 ^{0}C/S

100 ^{0}C/S

AMBIENT

PREHEAT

ACQUISITION

ANNEAL

TIME (SECONDS)
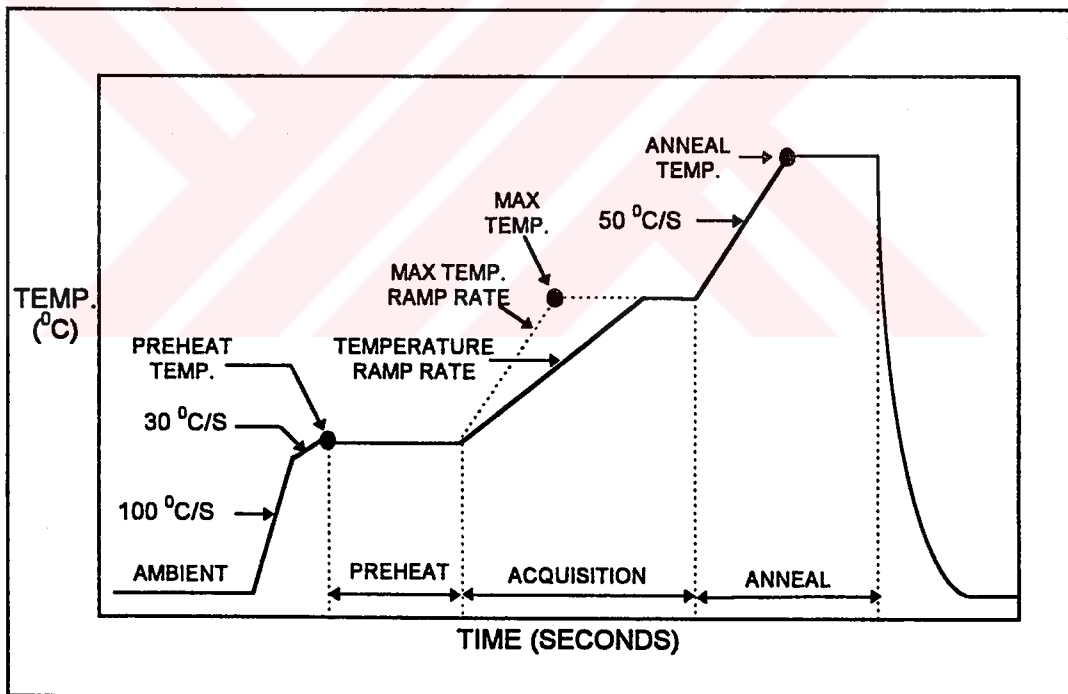
Figure 4. Typical time temperature profile (TTP).

CHAPTER 4

RESULTS AND DISCUSSION

The experiments were carried out to determine the effect of heating rate, dose rate, heat treatment and fading on the kinetic parameters in the glow curve of the $CaF_2:Dy$ (TLD-200). The results have been divided into four subsections. It was observed during the experiment that the pre-annealing up to 24 hours, had no perceptible effect on the glow curve of the TLD-200, therefore it is not included in discussion.

4.1 Effect of post-annealing on the Glow curve of TLD-200

The post annealing experiments were made for the temperature range of 30-250^{0}C with an step increase of 10 ^{0}C for two annealing times of 5 and 15 minutes. Figure 6 shows a typical glow curve of the TLD-200 sample exposed to $^{90}Sr-^{90}Y$ β-rays for 5 minutes after a standard annealing at 400 ^{0}C for 10 minutes.
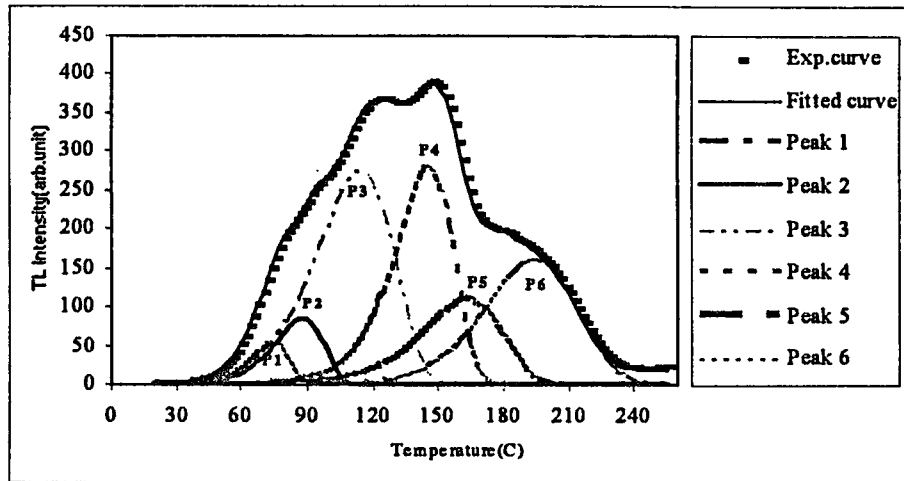
Figure 5 A typical glow curve of TLD-200 sample exposed to β-rays for 5 minutes after a standard annealing at 400 ^{0}C for 10 min.

As seen from figure 5, there are six peaks in the glow curve of TLD-200 in the investigated temperature range of 0-250 ^{0}C. However, it should be mentioned that there are other peaks in the glow curve of the TLD-200 existing of higher temperatures, i.e., above 250 ^{0}C. Since we wanted to investigate the glow curve in the temperature range of 0-250 ^{0}C, we only present the results for the six peaks of the glow curve of TLD-200. The effect of the post-annealing temperature on the glow curve of the TLD-200 are presented in the figures 6-11. As seen from these figures, as the post annealing temperature increases, the peaks appearing at low temperature disappear, and the total TL intensities also decrease. The main reason that the low temperature peaks disappear with increasing post-annealing temperature is that the traps or defect centers responsible for the appearance of these low temperature peaks are thermally bleached during post annealing treatment.

Figure 6   Glow curve of the TLD - 200 sample post annealed at 75^0C after

β-irradiation and read immediately.

Figure 7   Glow curve of the TLD - 200 sample post annealed at 89^0C after

β-irradiation and read immediately.
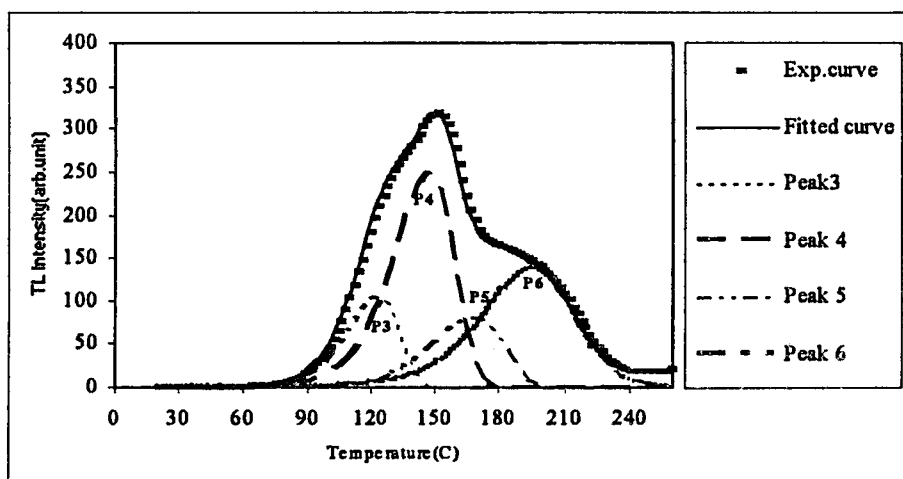
Figure 8 Glow curve of the TLD - 200 sample post annealed at 113^0C after

β -irradiation and read immediately.
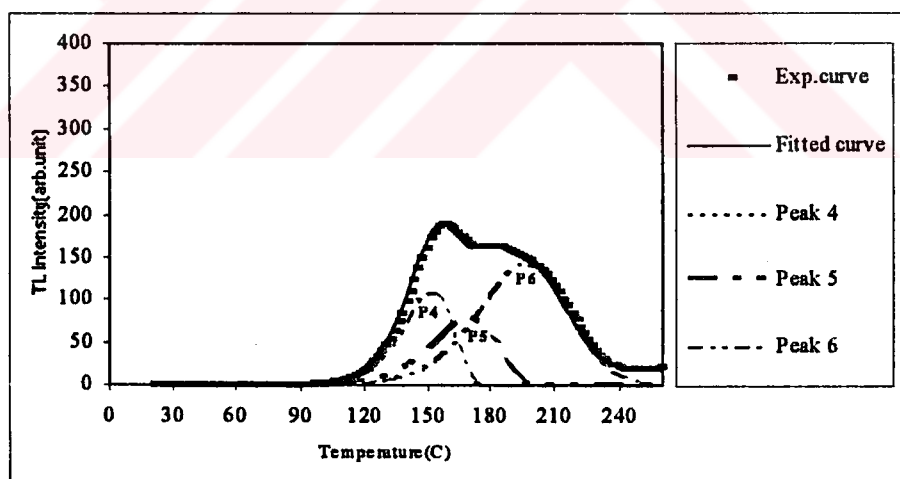
Figure 9 Glow curve of the TLD - 200 sample post annealed at 146^0C after

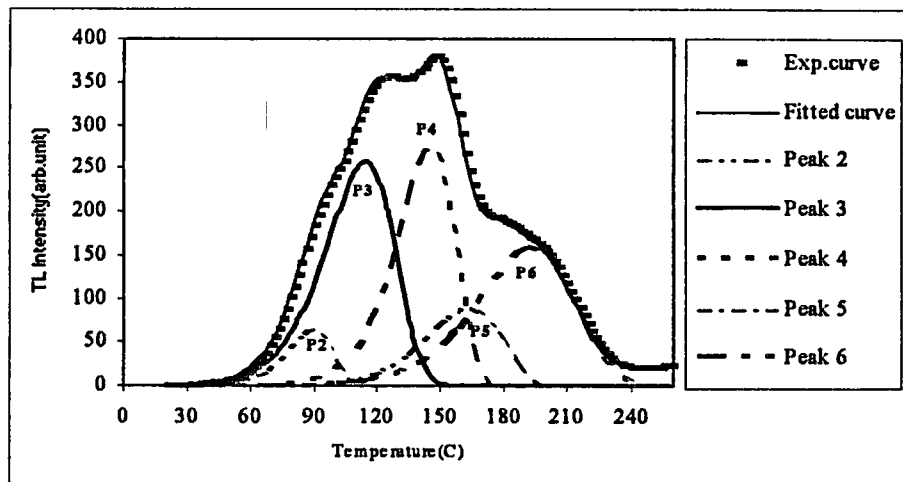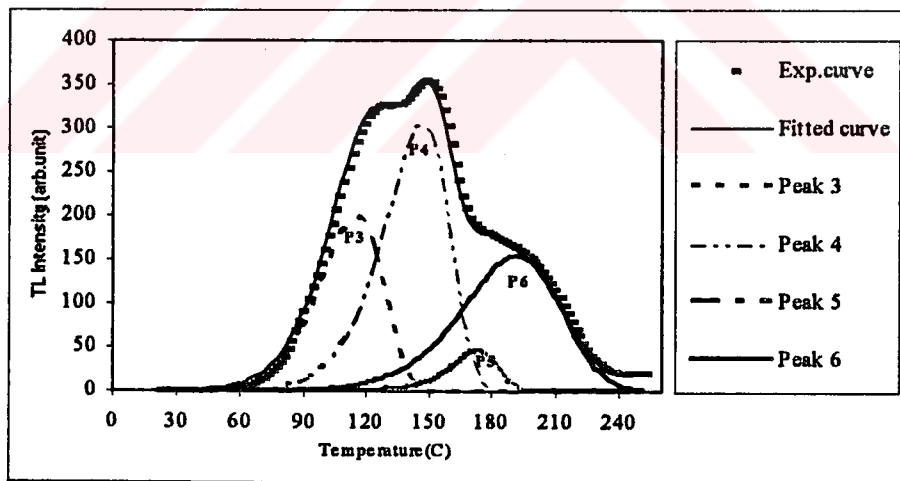β -irradiation and read immediately.
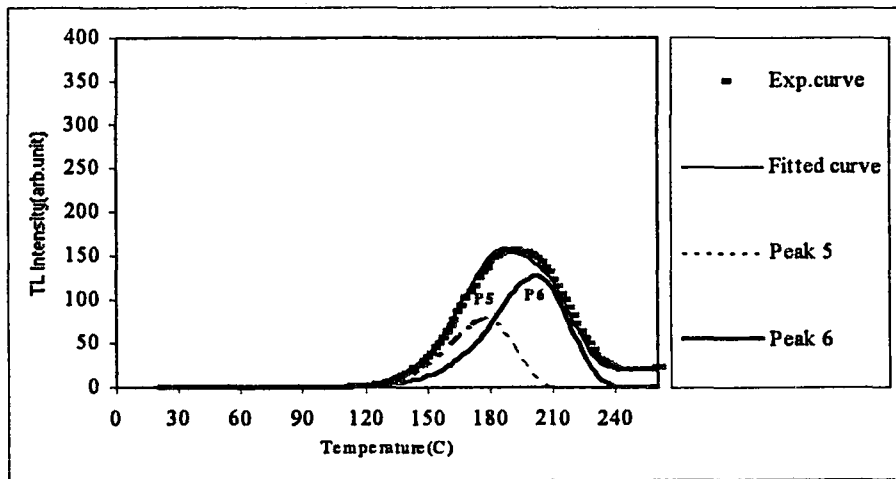
Figure 10 Glow curve of the TLD - 200 sample post annealed at 165^{0}C after β-irradiation and read immediately.
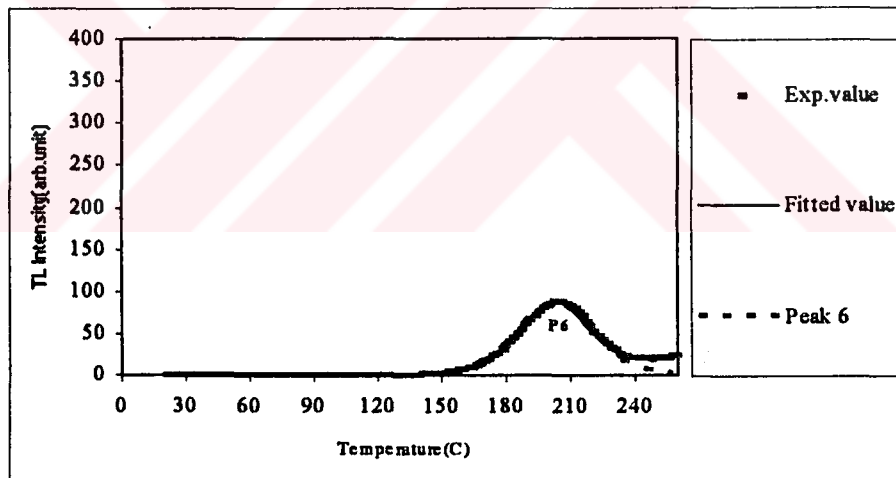
Figure 11 Glow curve of the TLD - 200 sample post-annealed at 195^{0}C after β-irradiation and read immediately.

4.1.1 Effects of 5 minute Post-annealing on glow curve of TLD-200 and its kinetic parameters

To see the effect of the post-annealing time on the glow curve and its kinetic parameters two sets of experiment were carried out. Here we present the results of 5 minute post-annealing on the glow curve of TLD-200 sample in figures 12-17.
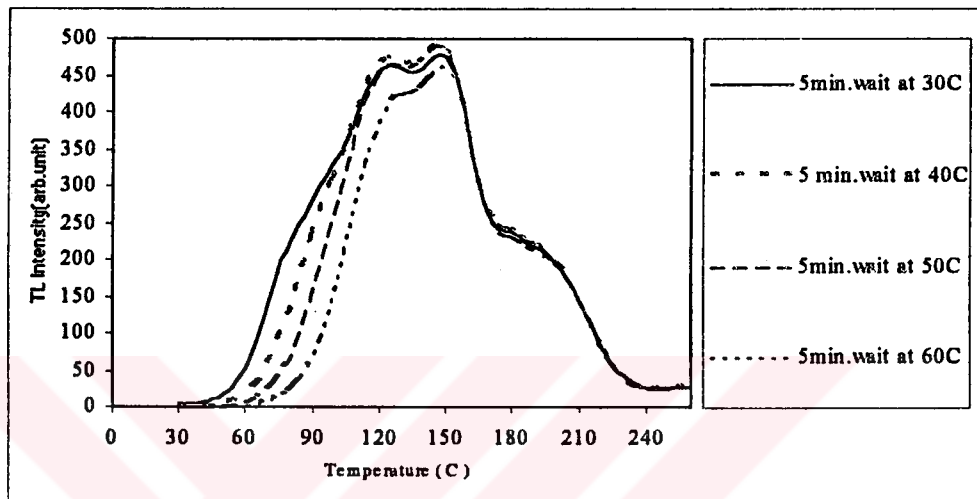
Figure12 Appearance of glow curve of TLD-200 after 5 minute post-annealing at 30 °C, 40 °C, 50 °C, and 60 °C.
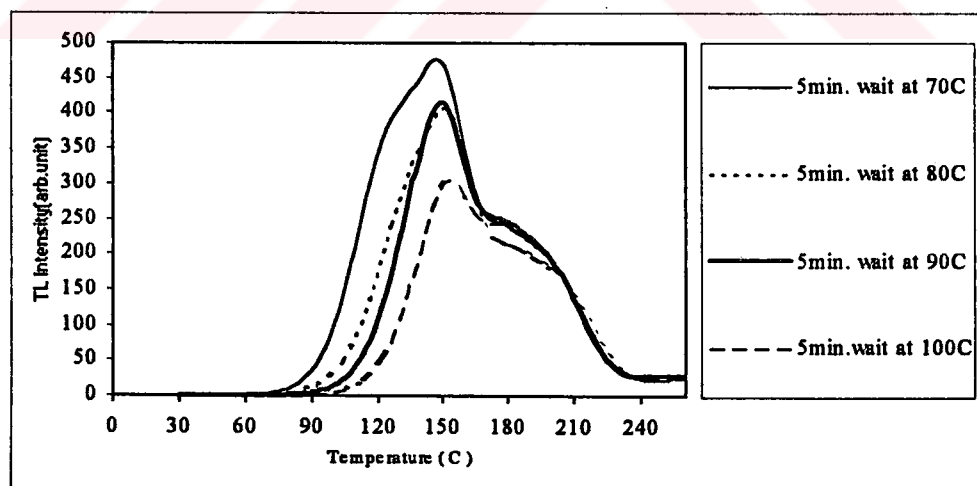
Figure13 Appearance of glow curve of TLD-200 after 5 minute post-annealing at 70 °C, 80 °C, 90°C, and 100 °C.
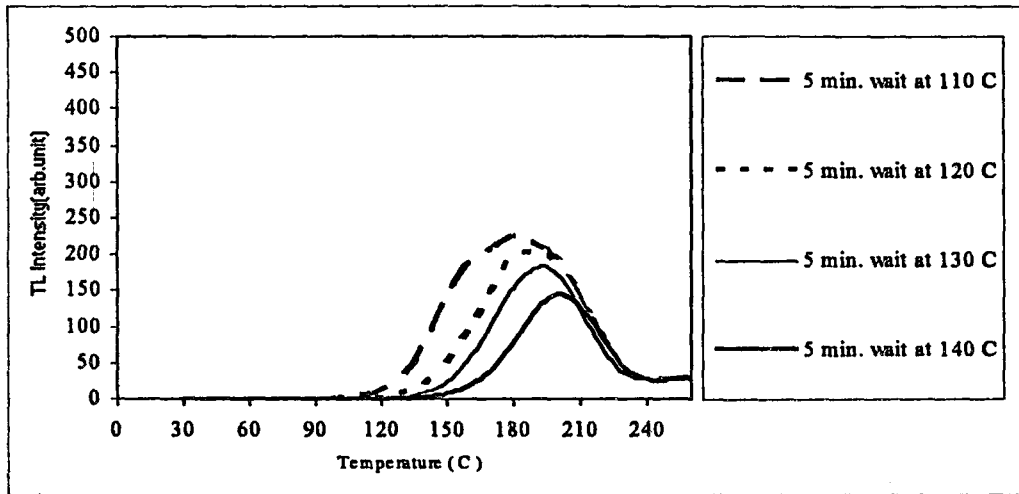
Figure14 Appearance of glow curve of TLD-200 after 5 minute post-annealing at

110 ^{0}C, 120 ^{0}C, 130^{0}C, and 140 ^{0}C.
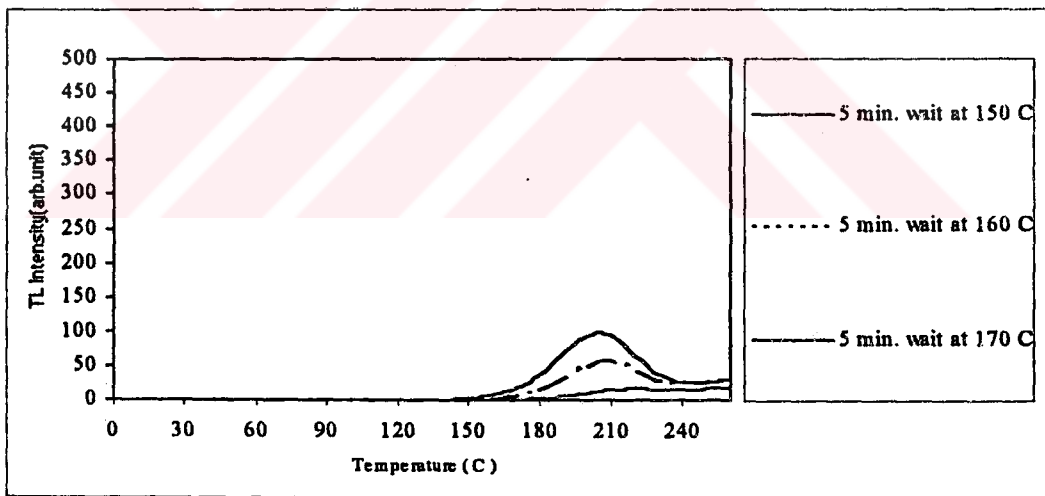
Figure15 Appearance of glow curve of TLD-200 after 5 minute post-annealing at

150 ^{0}C, 160 ^{0}C, and 170 ^{0}C.

The main effect of the five minute post annealing is that it results in a higher

decrease in the total intensity of the glow curve of TLD-200 and a faster decay in the low

temperature glow peaks as compared to the results of the immediate post-annealing (post-annealing with no waiting time).
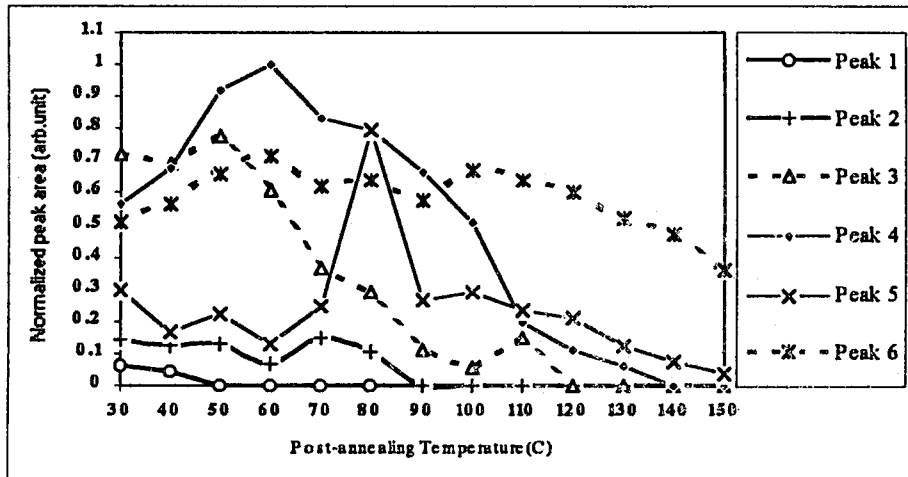
Figure 16 Effect of 5 minute post-annealing on the normalized peak areas of
TLD-200 (CaF$_2$:Dy) Crystal.

The changes in the normalized peak areas of the glow peaks as a function of post-annealing temperature are illustrated in figure 16. Post-annealing at different temperature made great changes on the areas of each peak. Peak 1 immediately decays out at temperature above 50 ^{0}C. A very slight change occurs in peak 2 up to temperature 80 ^{0}C, but after 80 ^{0}C it quickly dies out. Peak 3 first shows a slight increase up to 70 ^{0}C and then sharply decreases with increasing post-annealing temperature up to 100 ^{0}C. There seems an abnormal increase in the areas of peak 3 between 100 ^{0}C and 110 ^{0}C, and we think that it is mainly due to experimental error. Peak 4 first shows a quick rise up to 60 ^{0}C, and then continuously decreases with increasing temperature. A noticeable change takes place in peak 5. First it shows an up and down changes up to 70 ^{0}C, then shows very drastic increase and decrease between the temperatures 70 ^{0}C and 90 ^{0}C. Peak 6 first increases up to 60 ^{0}C, then it

also shows an up and down behavior between 60 ^{0}C and 100 ^{0}C, and then it slowly decreases with temperature. The variation in the activation energy of glow peaks of TLD-200 (CaF$_2$:Dy) crystal for 5 minute post-annealing is given in figure 17 (a) and (b).
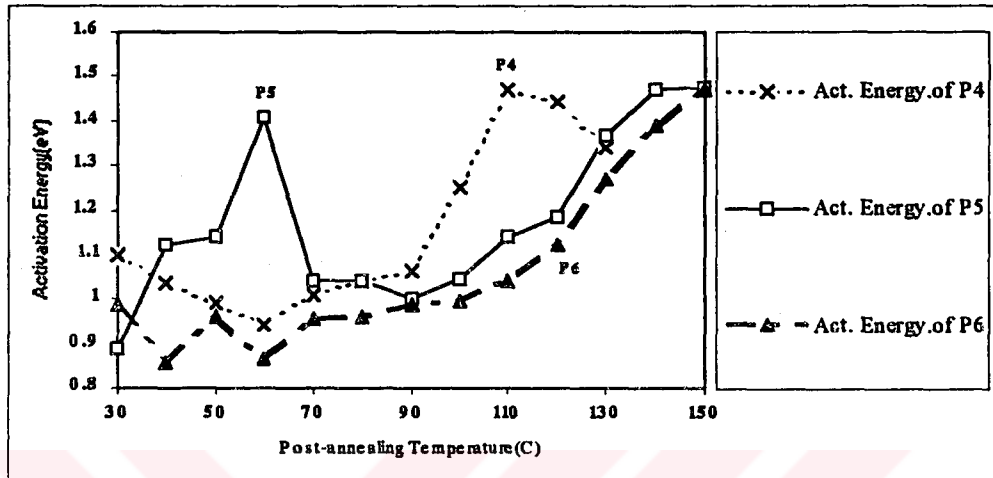
(b)
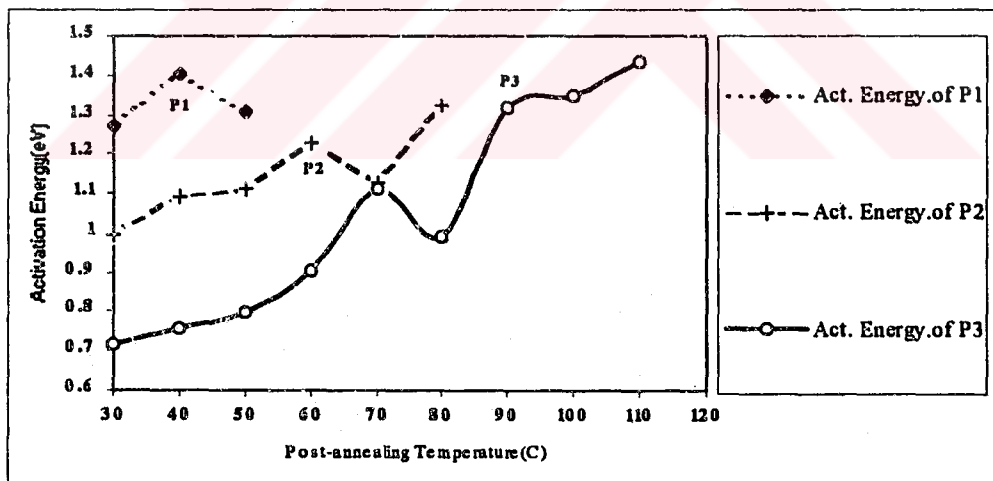
(a)

Figure 17 Effect of 5 minute post-annealing on the activation energy of the glow peaks of TLD-200 (CaF$_2$:Dy) crystal. **(a)** On the peaks 1,2, 3 and **(b)** on the peaks 4,5 and 6.

43

Activation energy of peak 1 first increases and then decreases. Since peak 1 decays out at the temperatures above 50 ^{0}C, there is no more data for peak 1 in figure 17 (a). The activation energy of peak 2 increases gradually up to 60 ^{0}C, then drops at 70 ^{0}C, and then quickly increases to its final point. There seems a general upward trend in peak 3 except that it shows a decline at the temperatures between 70 and 80 ^{0}C. As seen from figure 17 (b) peak 4 declines steadily until 60 ^{0}C, then increases with a small change in upward direction up to 90 ^{0}C, and continues to increase above this temperature but much faster until 110 ^{0}C, and then begins to decline again. Peak 5 increases severely up to 40 ^{0}C, then goes on steadily until 50 ^{0}C, and then shows a very drastic increase and decrease between 50 ^{0}C and 70 ^{0}C. Past 70 ^{0}C it shows a slight decrease up to 90 ^{0}C, and then monotonically increases with increasing temperature. The last value of activation energy for peak 5 is the same as the previous value. Peak 6 shows a zigzag pattern until 70 ^{0}C and then steadily increases up to 100 ^{0}C. Past 100 ^{0}C it quickly increases to its final value with a further increase in temperature.

4.1.2 Effects of 15 minute Post-annealing on glow curve of TLD-200 and its kinetic parameters

In this part we provide the results of the effect of 15 minute post-annealing on the glow curve of TLD-200 (CaF$_2$:Dy) and its kinetic parameters in figures 18-20.
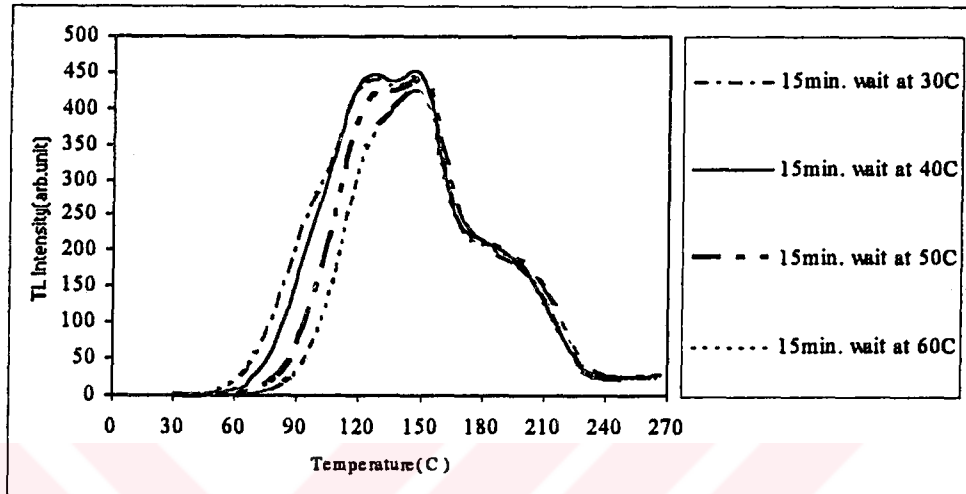
Figure18 Appearance of glow curve of TLD-200 after 15 minute post-annealing at 30 ^{0}C, 40 ^{0}C, 50 ^{0}C, and 60 ^{0}C.
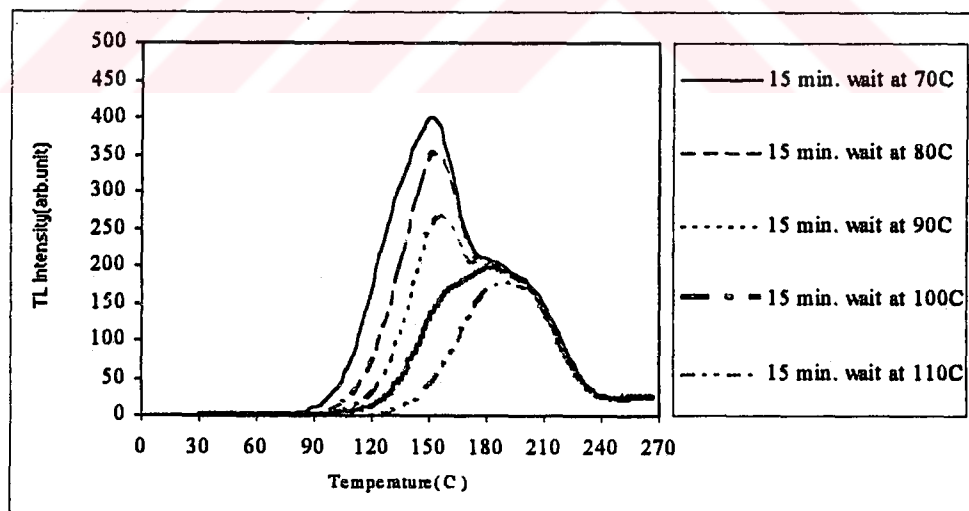
Figure19 Appearance of glow curve of TLD-200 after 15 minute post-annealing at 70 ^{0}C, 80 ^{0}C, 90 ^{0}C, 100 ^{0}C, and 110 ^{0}C.

45
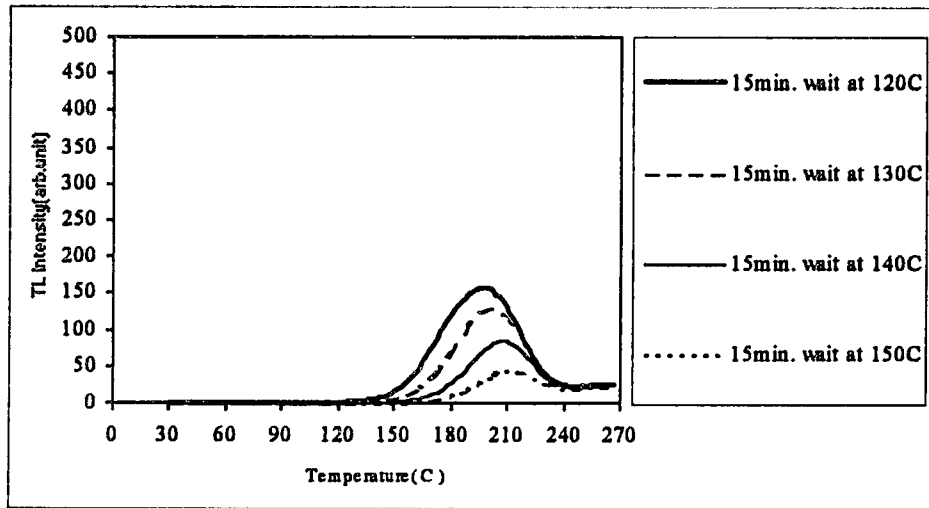
Figure 20 Appearance of glow curve of TLD-200 after 15 minute post-annealing at

120 ^{0}C, 130 ^{0}C, 140 ^{0}C, and 150 ^{0}C.

These figures and previous post-annealing results clearly indicate that the decrease in intensity of glow curve of CaF_2:Dy crystal gets larger and the low temperature glow peaks die out much faster as the post-annealing time prolongs. Effect of 15 minute post-annealing on normalized peak areas of TLD-200 is illustrated in figure 21.
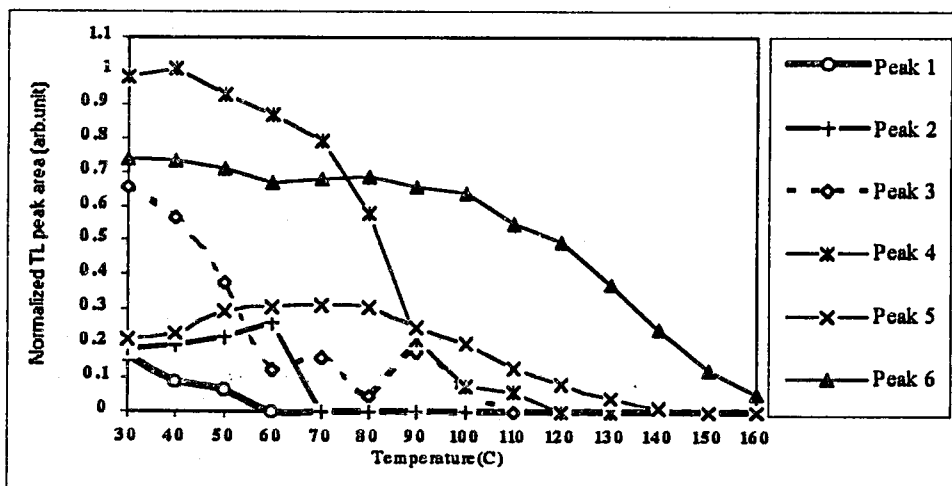
Figure 21 Effect of 15 minute post-annealing on the normalized peak areas of

TLD-200 (CaF$_2$:Dy) crystal.

All normalized TL peak areas except peaks 2 and 3 tend to decrease generally. First peak decreases smoothly. On the other hand, peak 2 increases gradually up to 60 ^{0}C, then drops to its minimum value with increasing post-annealing temperature. Third peak decreases steadily until 60 ^{0}C, then increases up to 70 ^{0}C, and then decreases and increases again. Past 80 ^{0}C it drops to its lowest value at 120 ^{0}C. One can see that the fourth peak, highest of all, has continuously downward tendency, although a small initial increase appears at about 40 ^{0}C. Past 40 ^{0}C, peak 4 decreases linearly until 70 ^{0}C. Its peak areas has a great slope between 70 ^{0}C and 90 ^{0}C. Above 90 ^{0}C it slowly decreases to its minimum value. Fifth peak shows a small increase up to 70 ^{0}C, then steadily decreases with increasing temperature. Peak six continuously decreases with increasing post-annealing temperature but decrease is much faster at temperatures above 100 ^{0}C.

The variation of activation energy of glow peaks of TLD-200 (CaF$_2$:Dy) crystal for 15 minute post-annealing is given in figure 22 (a) and (b). As shown in figure 22 (a), peak 1 first increases up to 40 ^{0}C then decreases with increasing temperature. Peak 2 sharply increases to its maximum value at about 60 ^{0}C. Peak 3 also quickly rises up to 60 ^{0}C and then goes to its maximum value with a zigzag behavior.

As seen from figure 22 (b), peak 4 and 6 shows a similar behavior. They both first increase with temperature to their maximum value and then decrease. Peak 5 first shows a decrease with temperature up to 60 ^{0}C and then continuously increases with a further increase in temperature.

47
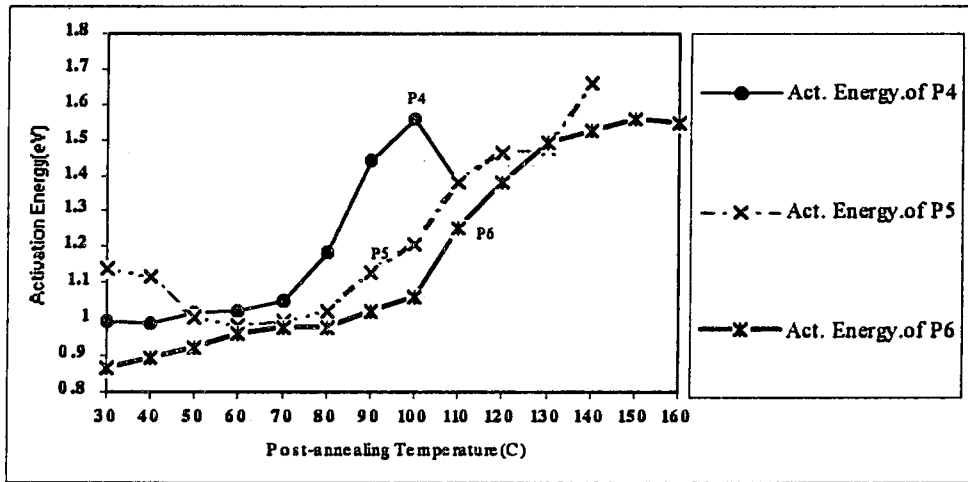
(b)
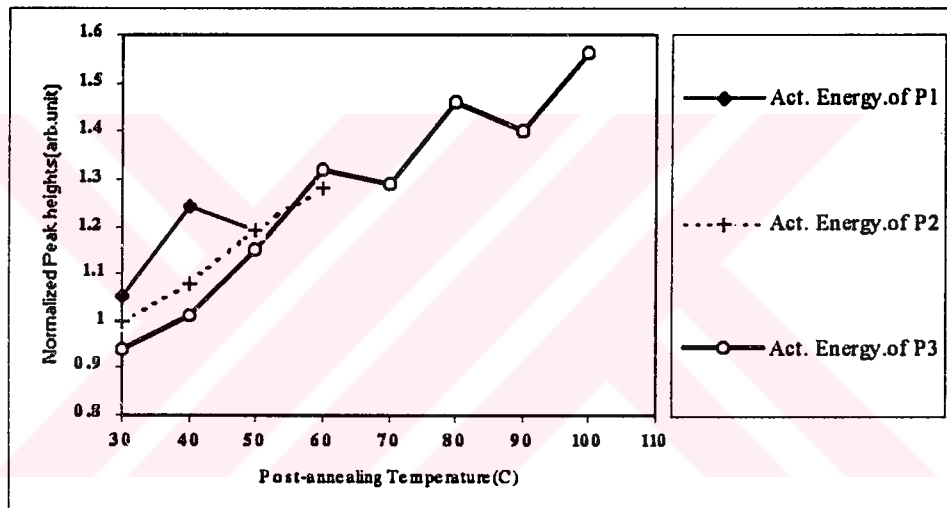
(a)

Figure 22 Effect of 15 minute post-annealing on the activation energy of the glow

peaks of TLD-200 (CaF$_2$:Dy) crystal. **(a)** On the peaks 1, 2, 3 and

(b) on the peaks 4,5 and 6.

4.2 Determination of kinetic parameters of glow Peak VI

Our CGCD deconvolution analysis of glow peaks of TLD-200 crystal has shown
that all the peaks except peak 6 obeyed the first order kinetics,i.e, their kinetic orders are
one. Since there have been no published studies about the kinetic order of peak 6 it has
become a significant part of the objective of this study to determine kinetic order and other
kinetic parameters of peak 6 in the glow curve of TLD-200. To determine the kinetic
parameters of peak 6 it is first necessary to separate peak 6 from other peaks. As seen
from the figures of post-annealing the low temperature peaks presented high instability. To
isolate the sixth glow peak we have used the method of Hoogenstraaten which consists of
thermal erasing of the low temperature peaks. In order to select the optimal thermal
treatment we have subjected the CaF$_2$:Dy (TLD-200) sample to different time range
from 1 minute to 25 minute at 145 ^{0}C (shown in figure 23). The criterion used to select the
thermal treatment to erase the low temperature glow peaks consisted in eliminating the
influence of this low temperature peaks with minimal loss of intensity in peak six.
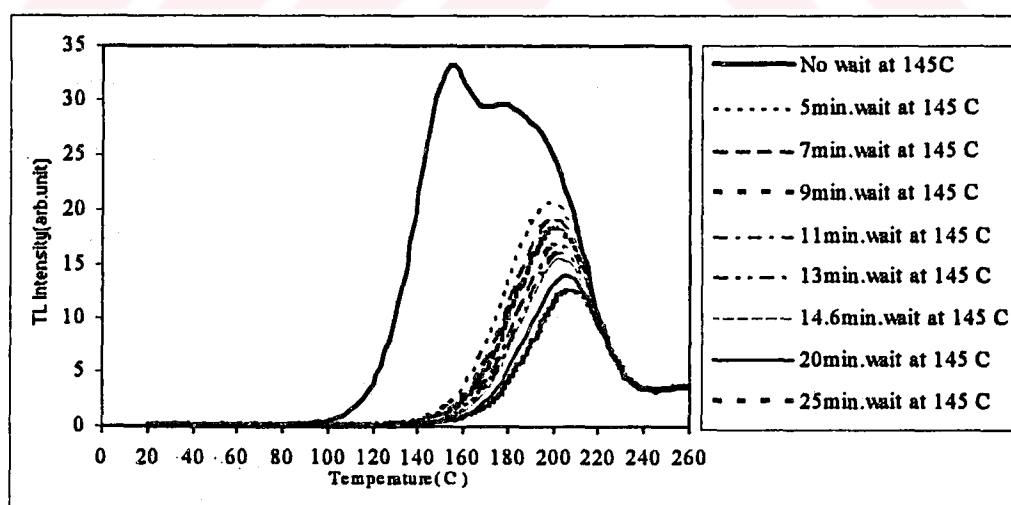
Figure 23   Thermal   treatments on the 6th peak.

Applying above criterion we have found that the post irradiation annealing at 145 ^{0}C for five minute effectively separate the peak VI from other peaks with minimum loss of intensity. To determine the TL parameters we have used isothermal, initial rise and peak shape method along with CGCD computer program.

The initial rise method does not require an explicit knowledge of the order of kinetics obeyed in the process, while as the other methods require one to know the order of kinetics.

4.2.1 Determination of kinetic order of glow peak VI

To determine the b value by isothermal decay method, irradiated samples were placed in an oven at controlled temperatures $T_1 = 463.15 \pm 1$ K, $T_2 = 468.15 \pm 1$ K, $T_3 = 473.15 \pm 1$ K, $T_4 = 478.15 \pm 1$ K, $T_5 = 483.15 \pm 1$ K during the same time period (3 seconds). By measuring the areas of the subsequently obtained glow curves and plotting $I^{(1-1/b)}$ vs. t we have tried various values of b, choosing as the correct value the one giving a straight line plot, as shown in figures 24,25,26,27,28. It is very hard to determine the exact value of the kinetic order of peak VI. Since all the curves show a similar behavior.
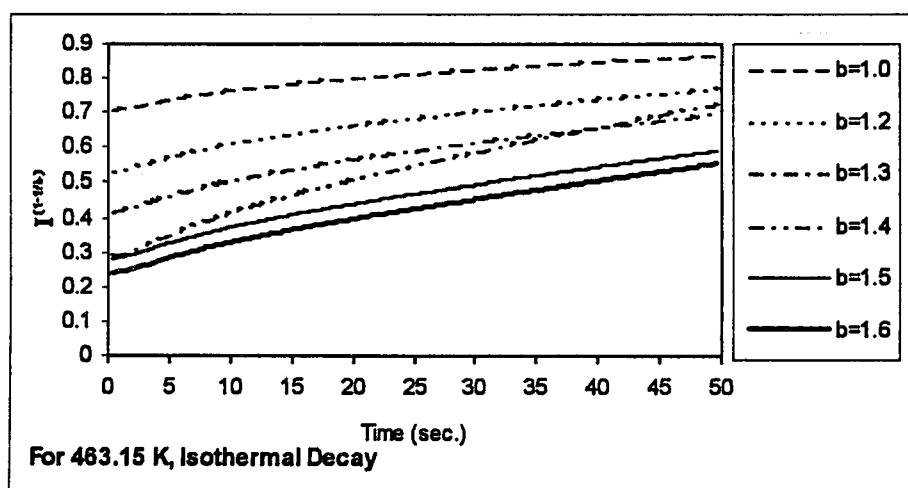
Figure 24   Isothermal Decay of   peak VI at 463.15 K.

For 468.15 K, Isothermal Decay
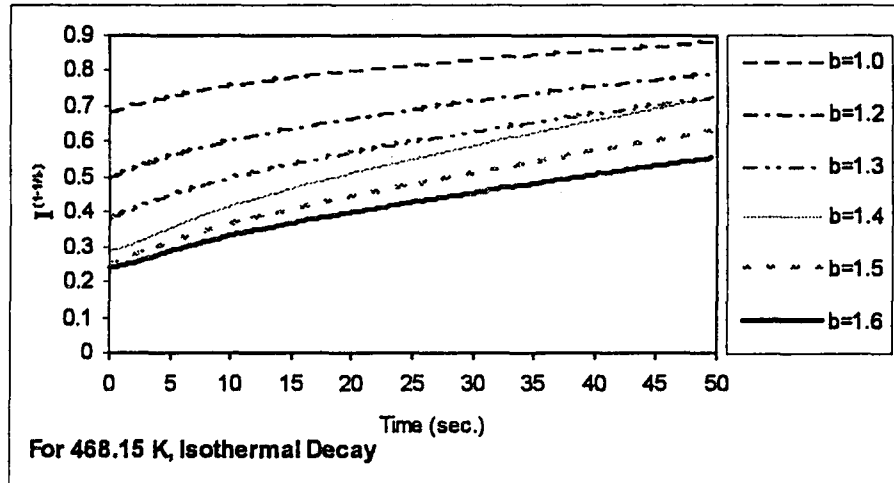
Figure 25   Isothermal Decay of **peak VI** at 468.15 K.

For 473.15 K, Isothermal Decay
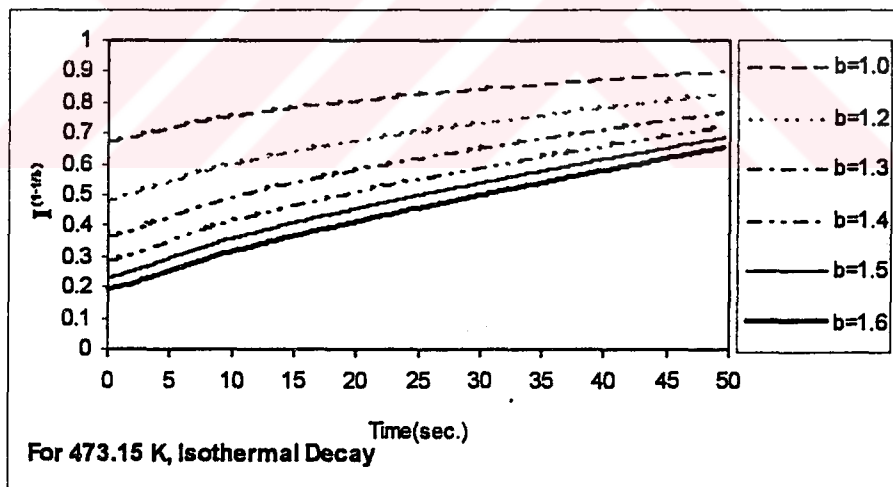
Figure 26   Isothermal Decay of **peak VI** at 473.15 K.

51
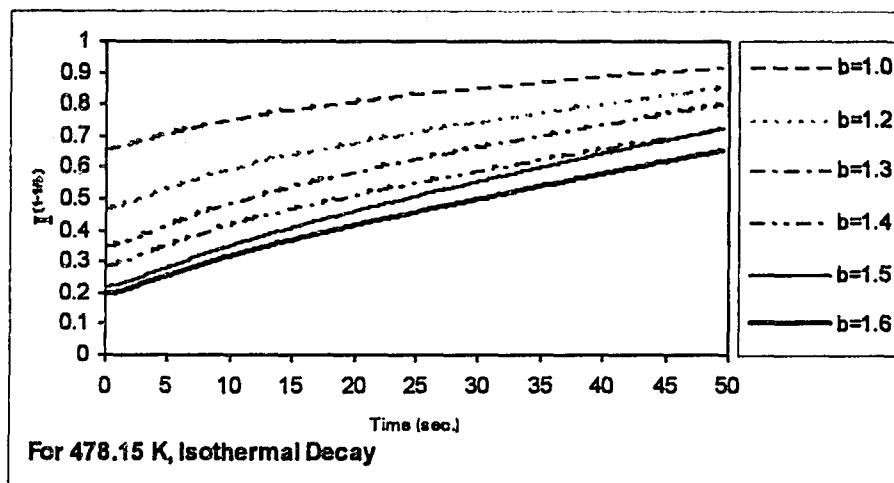
Figure 27   Isothermal   Decay   of   6th peak   at   478.15 K.
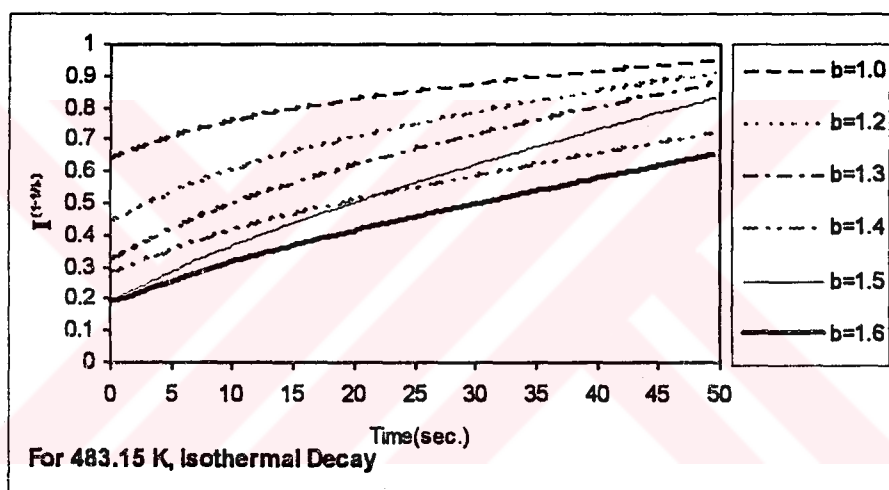
Figure 28   Isothermal   Decay   of   6th peak   at   483.15 K.

It is also seen from these figures that however, the isothermal decay curve with the kinetic order b=1.6 gives a better straight line at all the temperature. The actual estimate of the kinetic order (**b** or *l*) of peak VI will be made together with the aid of the isothermal decay curve and calculated the peak shape parameters to be discussed in the section 4.2.2 and 4.2.3.

4.2.2 Peak parameters for the peak VI by peak shape method:

In this method the following formulas were used and their values were obtained from the glow curves of peak VI. Then the calculated peak shape parameters and kinetic parameters are tabulated in Tables 1 and 2, respectively.

$$\omega = T_2 - T_1, \qquad \delta = T_2 - T_m, \qquad \tau = T_m - T_1,, \qquad \mu_g = \delta/\omega$$

$$E_\omega = [2.52 + 10.2(\mu_g - 0.42)]\frac{kT_m^2}{\omega} - 2kT_m, \quad E_\delta = [0.976 + 7.3(\mu_g - 0.42)]\frac{kT_m^2}{\delta},$$

$$E_\tau = [1.51 + 3(\mu_g - 0.42)]\frac{kT_m^2}{\tau} - [1.58 + 4.2(\mu_g - 0.42)]2kT_m, \text{ and frequency factor}$$

formula :

$$s = \frac{\beta E}{kT_m^2}\left[\exp\left(-\frac{E}{kT_m}\right)\left(1 + (b-1)\frac{2kT_m}{E}\right)\right]^{-1} \text{ [24]}.$$

It is known that there is a relation between the shape factor and the kinetic order b. The values of the kinetic order as a function of peak shape factor, μ_g , are tabulated in Table 3. The value of geometric factor or shape factor μ_g is found to be between 0.45 and 0.50, as seen from Table 1. Its mean value is about 0.48 . The kinetic order corresponding to the mean value of the shape factor is about 1.55.

53

Hence comparing the results obtained from the peak shape method with the isothermal decay method, we can confidently claim that the kinetic order of peak VI is between 1.55 and 1.60.

Table 1 Chen's peak parameters for the sixth peak.

	Low-temperature half width $T_1(K)$	Peak-temperature at maximum $T_m(K)$	High-temperature half width $T_2(K)$	ω, $\omega=T_2-T_1$ (K)	δ, $\delta=T_2-T_m$ (K)	τ, $\tau=T_m-T_1$ (K)	Geometrical factor, $\mu_g=\delta/\omega$
For experimental data							
For 5 min. wait.	447.95	472.15	493.44	45.497	21.292	24.205	0.47
For 7 min. wait.	450.93	472.15	493.95	43.024	21.801	21.223	0.50
For 9 min. wait.	452.53	474.15	495.14	42.602	20.984	21.618	0.49
For 11 min. wait.	452.85	474.15	495.13	42.279	20.975	21.304	0.49
For 13 min. wait.	454.16	476.15	495.81	41.646	19.656	21.989	0.47
For 14.6 min.wait.	454.70	476.15	496.00	41.305	19.855	21.450	0.48
For 20 min. wait.	457.39	478.15	498.22	40.829	20.070	20.759	0.49
For 25 min. wait.	458.56	480.15	498.95	40.387	18.800	21.587	0.46
For fitted data							
For 5 min. wait.	449.87	472.15	492.86	42.986	20.708	22.278	0.48
For 7 min. wait.	450.58	472.15	493.59	42.999	21.437	21.562	0.49
For 9 min. wait.	452.60	474.15	494.44	41.839	20.292	21.547	0.48
For 11 min. wait.	453.57	474.15	494.41	40.838	20.259	20.579	0.49
For 13 min. wait.	454.73	476.15	494.99	40.258	18.843	21.416	0.47
For 14.6 min.wait.	457.09	476.15	495.05	37.965	18.905	19.060	0.49
For 20 min. wait.	457.75	478.15	495.07	37.137	16.917	20.396	0.45
For 25 min. wait.	458.81	478.15	496.82	38.016	18.671	19.345	0.49

Table 2 Kinetic parameters of peak VI calculated by Chen's method[48].

	For experimental data		For fitted data	
	E(eV)	s(s^{-1})	E(eV)	s(s^{-1})
For 5 min. wait.				
Chen(ω)	1.1897	7.685*10^{13}	1.3267	2.002*10^{15}
Chen(δ)	1.1971	9.130*10^{13}	1.3239	1.876*10^{15}
Chen(τ)	1.1681	4.597*10^{13}	1.2316	1.429*10^{15}
For 7 min. wait.				
Chen(ω)	1.4393	2.940*10^{16}	1.4029	1.234*10^{16}
Chen(δ)	1.4183	1.783*10^{16}	1.3889	8.839*10^{15}
Chen(τ)	1.4445	3.339*10^{16}	1.4003	1.160*10^{16}
For 9 min. wait.				
Chen(ω)	1.4013	1.035*10^{16}	1.3927	8.431*10^{15}
Chen(δ)	1.3906	8.030*10^{15}	1.3854	7.085*10^{15}
Chen(τ)	1.3948	8.865*10^{15}	1.3821	6.555*10^{15}
For 11 min. wait.				
Chen(ω)	1.4293	2.013*10^{16}	1.4824	7.136*10^{16}
Chen(δ)	1.4152	1.439*10^{16}	1.4650	4.709*10^{16}
Chen(τ)	1.4261	1.866*10^{16}	1.4817	7.015*10^{16}
For 13 min. wait.				
Chen(ω)	1.3494	2.648*10^{15}	1.3792	5.360*10^{15}
Chen(δ)	1.3478	2.549*10^{15}	1.3761	4.981*10^{15}
Chen(τ)	1.3340	1.835*10^{15}	1.3633	3.677*10^{15}
For 14.6 min.wait.				
Chen(ω)	1.4032	9.455*10^{15}	1.6245	1.803*10^{18}
Chen(δ)	1.3968	8.132*10^{15}	1.5973	9.445*10^{17}
Chen(τ)	1.3911	7.100*10^{15}	1.6316	2.151*10^{18}
For 20 min. wait.				
Chen(ω)	1.4863	5.865*10^{16}	1.4285	1.499*10^{16}
Chen(δ)	1.4714	4.125*10^{16}	1.4030	1.255*10^{16}
Chen(τ)	1.4823	5.341*10^{16}	1.4140	1.067*10^{16}
For 25 min. wait.				
Chen(ω)	1.3855	4.780*10^{15}	1.6002	8.657*10^{17}
Chen(δ)	1.3828	4.477*10^{15}	1.5784	5.171*10^{17}
Chen(τ)	1.3692	3.251*10^{15}	1.6009	8.812*10^{17}

Table 3 The kinetic order (b or l)versus μ_g

b	μ	b	μ	b	μ	b	μ
1.01	0.41867116	1.26	0.45097917	1.51	0.4770717	1.76	0.4988977
1.02	0.42011985	1.27	0.45212552	1.52	0.4780169	1.77	0.4997002
1.03	0.42155371	1.28	0.45326223	1.53	0.4789557	1.78	0.5004977
1.04	0.42297268	1.29	0.45438957	1.54	0.4798879	1.79	0.5012904
1.05	0.42437744	1.3	0.45550752	1.55	0.4808136	1.8	0.5020785
1.06	0.42576792	1.31	0.45661644	1.56	0.4817329	1.81	0.5028617
1.07	0.42714466	1.32	0.45771624	1.57	0.4826459	1.82	0.5036404
1.08	0.4285078	1.33	0.4588073	1.58	0.4835528	1.83	0.5044145
1.09	0.42985752	1.34	0.45988954	1.59	0.4844535	1.84	0.505184
1.1	0.43119425	1.35	0.46096325	**1.6**	**0.4853481**	1.85	0.5059491
1.11	0.4325181	1.36	0.46202846	1.61	0.4862368	1.86	0.5067096
1.12	0.43382927	1.37	0.46308544	1.62	0.4871195	1.87	0.5074658
1.13	0.43512807	1.38	0.46413408	1.63	0.4879964	1.88	0.5082176
1.14	0.43641478	1.39	0.46517466	1.64	0.4888677	1.89	0.5089652
1.15	0.43768947	1.4	0.46620729	1.65	0.4897331	1.9	0.5097085
1.16	0.43895246	1.41	0.46723207	1.66	0.490593	1.91	0.5104475
1.17	0.44020386	1.42	0.46824909	1.67	0.4914473	1.92	0.5111824
1.18	0.44144394	1.43	0.46925847	1.68	0.4922962	1.93	0.5119132
1.19	0.44267295	1.44	0.47026034	1.69	0.4931397	1.94	0.5126399
1.2	0.44389096	1.45	0.47125487	1.7	0.4939778	1.95	0.5133626
1.21	0.44509824	1.46	0.47224197	1.71	0.4948106	1.96	0.5140812
1.22	0.44629488	1.47	0.47322193	1.72	0.4956382	1.97	0.514796
1.23	0.44748115	1.48	0.47419477	1.73	0.4964607	1.98	0.5155068
1.24	0.44865716	1.49	0.47516061	1.74	0.4972781	1.99	0.5162138
1.25	0.44982315	1.5	0.47611953	1.75	0.4980903	2	0.5169169

4.2.3 Peak parameters for the peak VI by Initial rise method and CGCD computer program:

For the initial rise method, we have used initial part being 5% of maximum thermoluminescence intensity of the region where $T \ll T_m$ of glow curves. In addition, we have determined the peak parameters of sixth peak by means of CGCD computer program. The values of the activation energies and the frequency factors obtained by utilizing the initial rise method and CGCD programming are given in Table 4.

Table 4 Activation Energies and Frequency Factors founded by Initial

rise method and CGCD Program.

	For Initial Rise E(eV)	For CGCD Prog. E(eV)	For CGCD Prog Freq. Factor(s^{-1})
For 5 min. wait.	1.250	1.266	$2.18*10^{12}$
For 7 min. wait.	1.388	1.319	$7.46*10^{12}$
For 9 min. wait.	1.407	1.368	$2.35*10^{13}$
For 11 min. wait.	1.385	1.407	$6.03*10^{13}$
For 13 min. wait.	1.402	1.420	$8.81*10^{13}$
For 14.6 min.wait.	1.418	1.446	$1.51*10^{14}$
For 20 min. wait.	1.423	1.469	$1.51*10^{14}$
For 25 min. wait.	1.426	1.491	$3.57*10^{14}$

As we see from the Tables 2 and 4, the values of the activation energies obtained by three different methods are in rather good agreement. The maximum difference between the values calculated by three difference methods is less than 8 %, which is reasonably low value.

4.4 The Effects of different heating rate on glow curve of TLD-200 (CAF2:Dy) and its kinetic parameters

A series of experiments was carried out to investigate the effect of different heating rate on glow curve of TLD - 200 (CaF_2 :Dy) crystal and its kinetic parameters. In this part we used the CGCD deconvolution program to analyze the glow curves and to evaluate the kinetic parameters. In this method, the exposed samples were read out at different heating rate, such as 1, 3, 5, 7, 9, 11, 15, 17 and 19 $Ksec^{-1}$. Then the data gathered was analyzed by the CGCD. At each step of the process we have tried to get more precise fits to prevent underestimating or overestimating. The evaluated results and the appearance of glow curves of TLD-200 (CaF_2 :Dy) sample for each heating rate are presented in figures 29-38.
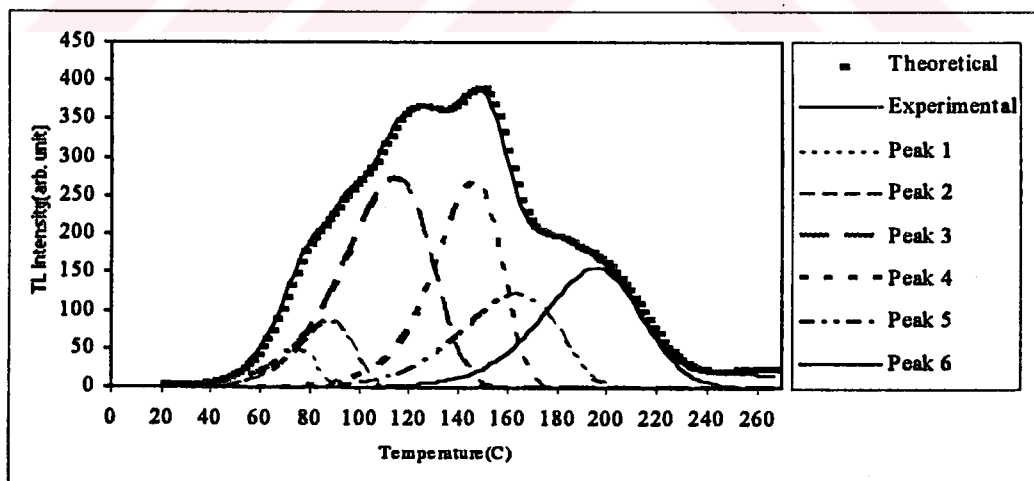
Figure 29 The appearance of deconvoluted glow curve of TLD-200 (CaF_2 :Dy) at heating rate 1 $Ksec^{-1}$.
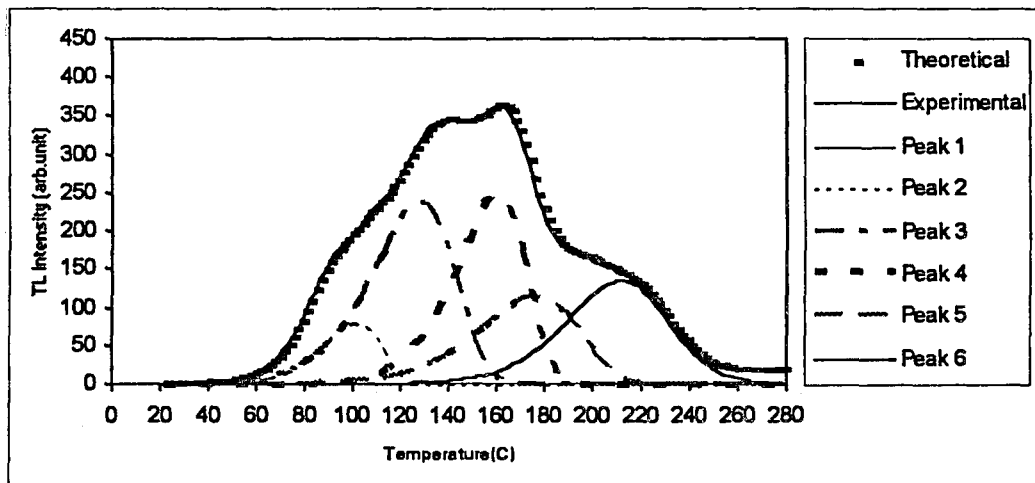
Figure 30 The appearance of deconvoluted glow curve of TLD-200 (CaF$_2$:Dy) at heating rate 3 Ksec^{-1}.
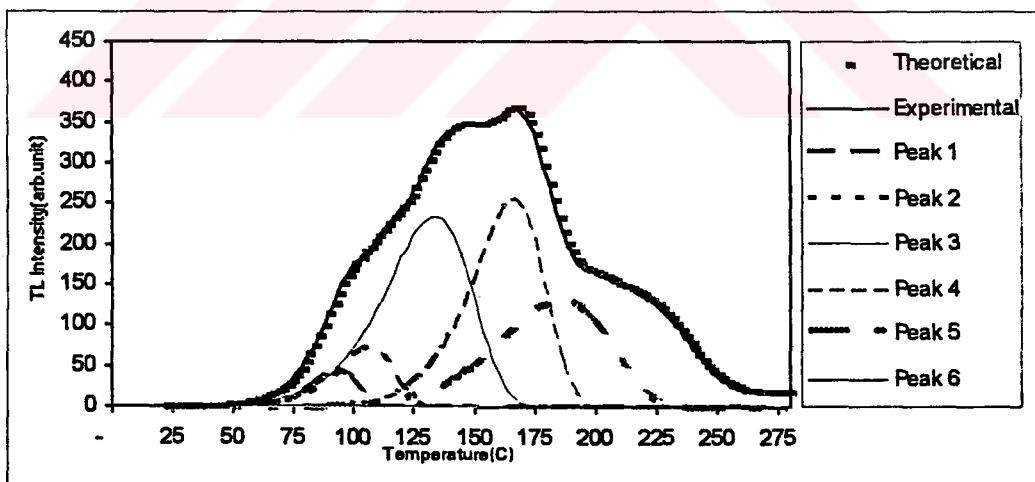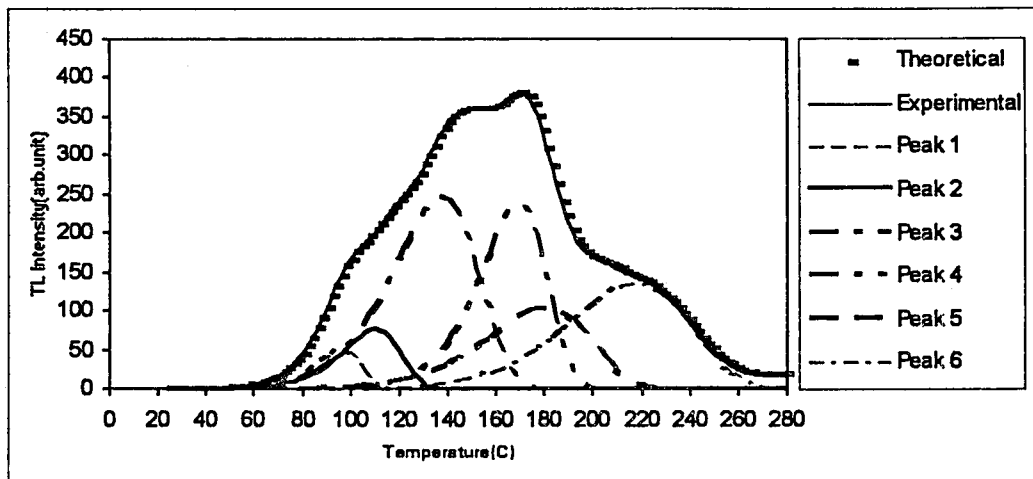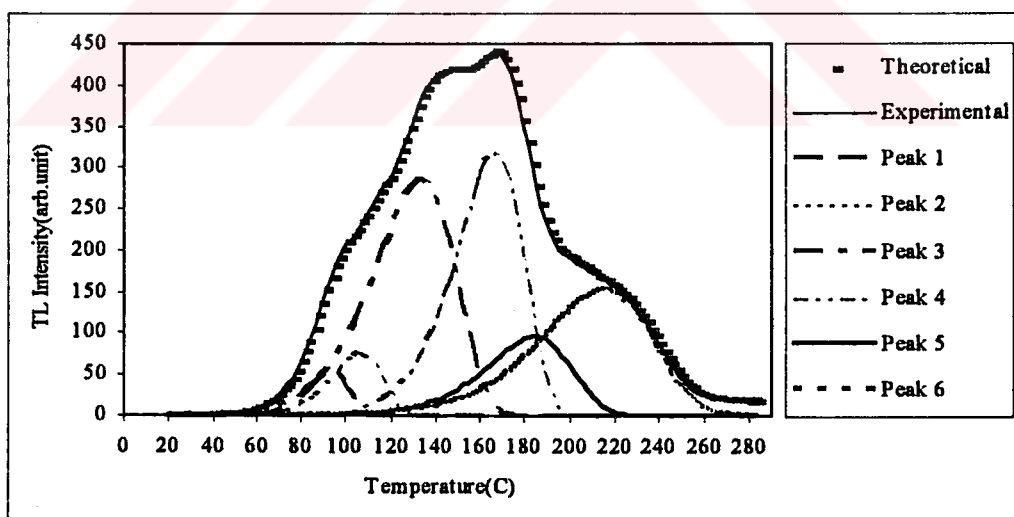

Figure 31 The appearance of deconvoluted glow curve of TLD-200 (CaF$_2$:Dy) at heating rate 5 Ksec^{-1}.

Figure 32 The appearance of deconvoluted glow curve of TLD-200 (CaF$_2$:Dy) at

heating rate 7 Ksec^{-1}.

Figure 33 The appearance of deconvoluted glow curve of TLD-200 (CaF$_2$:Dy) at
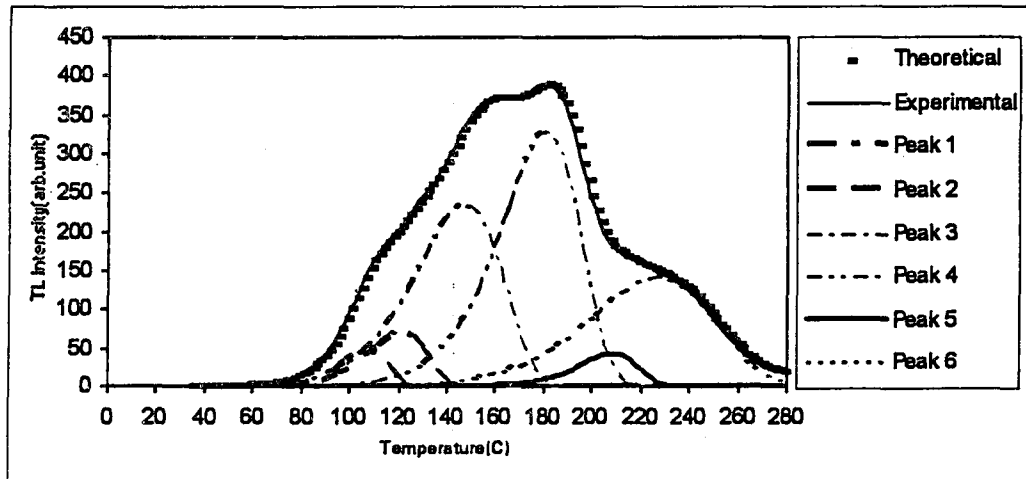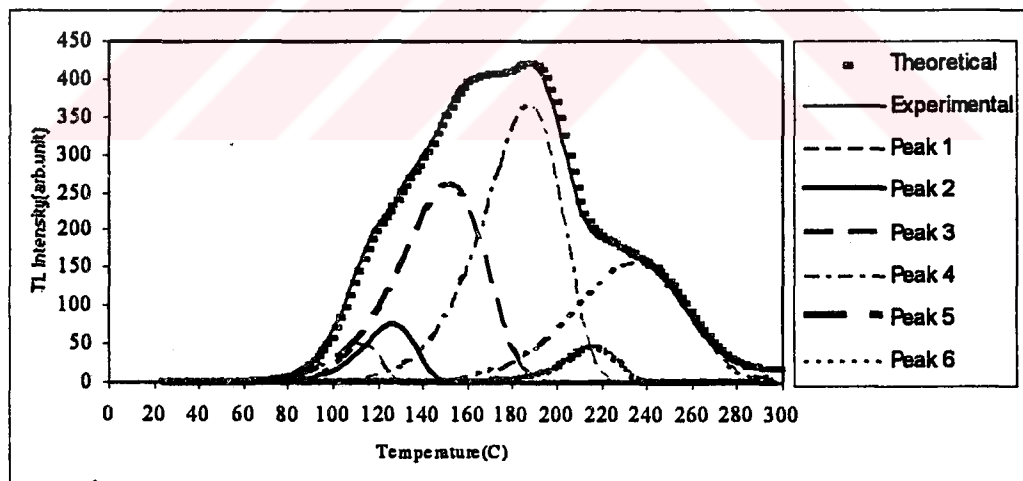
heating rate 9 Ksec^{-1}.

Figure 34 The appearance of deconvoluted glow curve of TLD-200 (CaF$_2$:Dy) at

heating rate 11 Ksec^{-1}.

Figure 35 The appearance of deconvoluted glow curve of TLD-200 (CaF$_2$:Dy) at
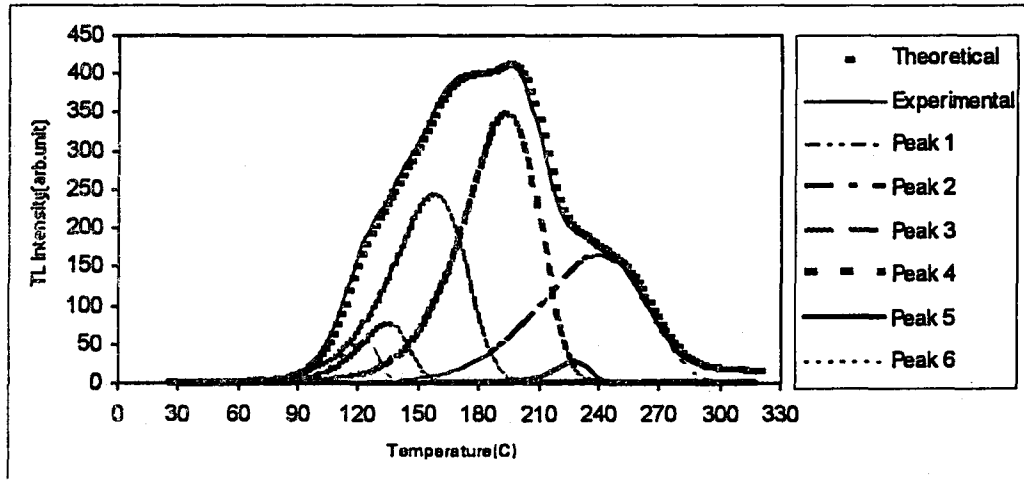
heating rate 13 Ksec^{-1}.

Figure 36 The appearance of deconvoluted glow curve of TLD-200 (CaF$_2$:Dy) at heating rate 15 Ksec^{-1}.

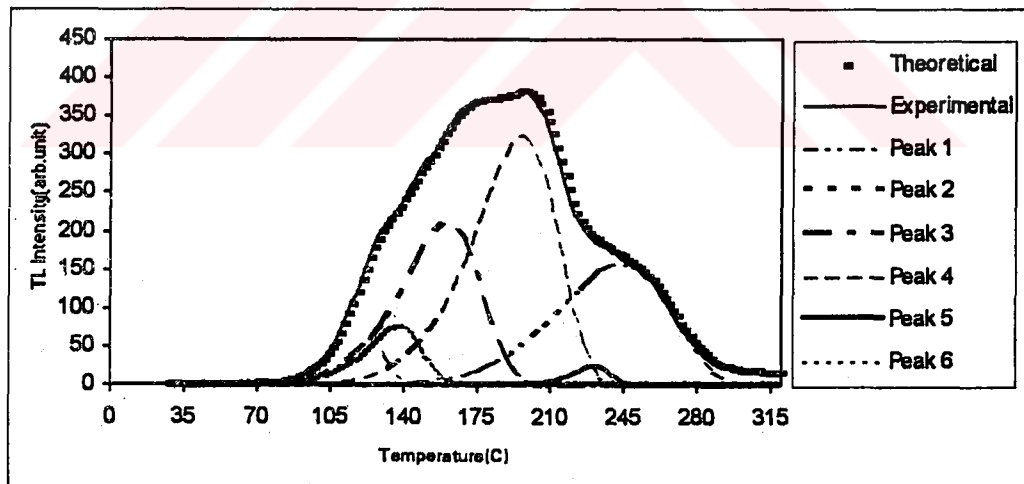**Figure 37** The appearance of deconvoluted glow curve of TLD-200 (CaF$_2$:Dy) at heating rate 17 Ksec^{-1}.

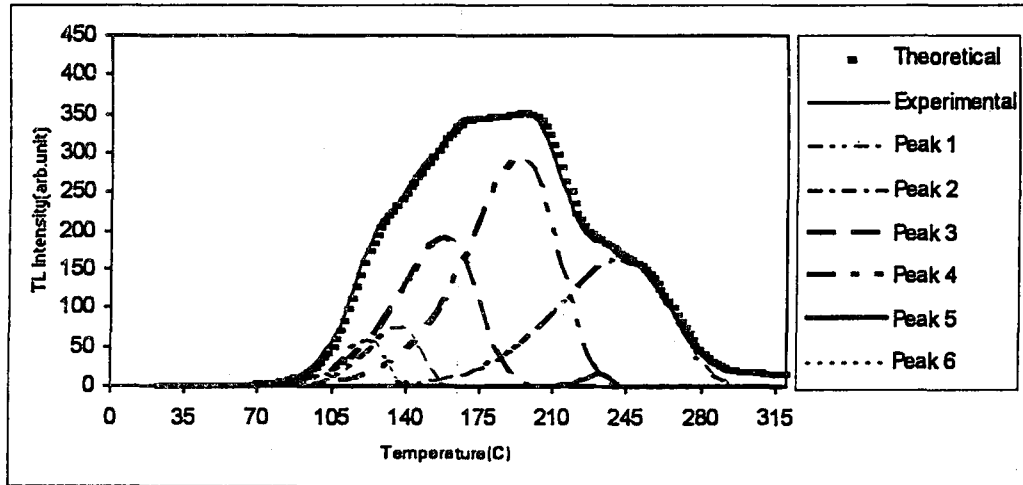**Figure 38** The appearance of deconvoluted glow curve of TLD-200 (CaF$_2$:Dy) at

heating rate 19 Ksec^{-1} .

Figures 29-38 represent the thermoluminescence intensity vs. temperature for

TLD-200 crystal at different heating rates. There are several points that can be made

about the effect of heating rate on TL glow curves. One is the change in the peak

heights with heating rate. Second effect is that the appearance of all the peaks occur

at higher temperatures. Another point is that the appearance or the shape of the glow

curves seems to be unaffected by heating rate. This indicates that heating rate does

not cause an interaction between defect centers or traps.

Figure 39 illustrates the variation of peak areas of the TL glow peaks as a

function of heating rate. It is clearly seen from figure 39(a). All three peaks (1,2,3)

show a similar behavior. They all first slightly decreases with heating rate up to 9 Ks^{-1} and then seem to level off at higher heating rate. Peak 4 and 6 also show a similar pattern. Both first decrease noticeably, then slightly increase, and then redecrease very
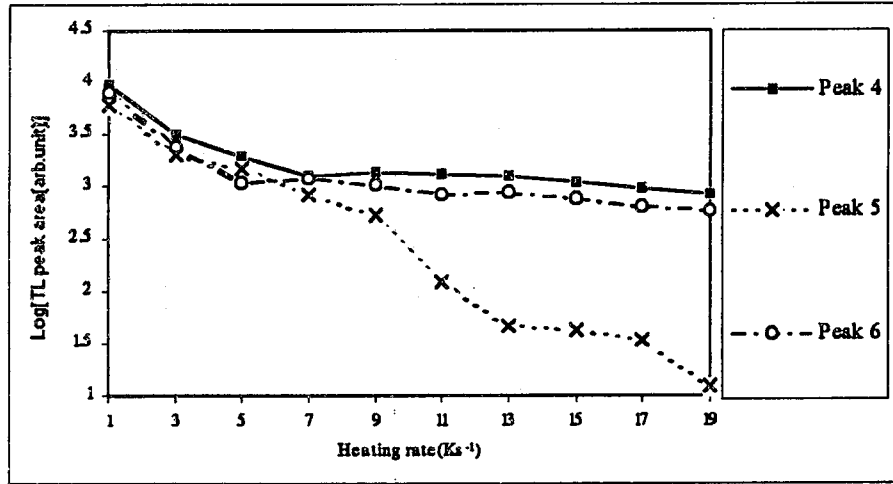

(b)
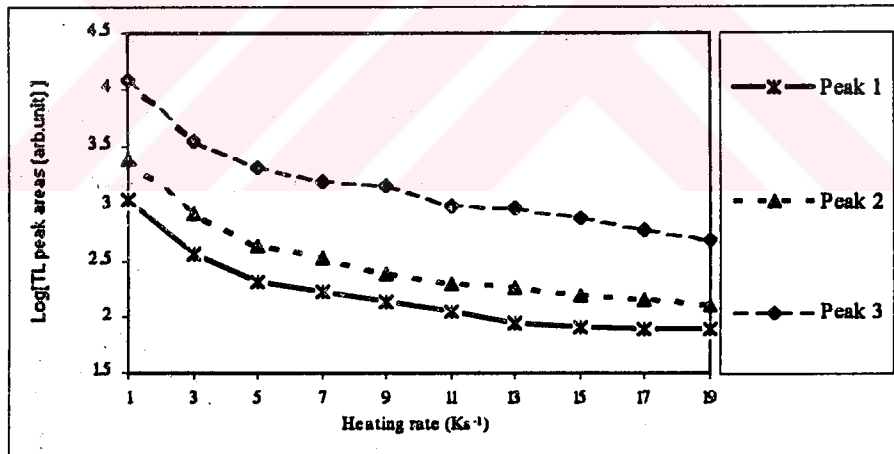
(a)

Figure 39 Variation of Logarithmic TL glow peak areas as a function of heating rate(Ks^{-1}) of TLD-200 (CaF$_2$:Dy) crystal. **(a)** For peaks 1, 2, 3 and **(b)** for peaks 4, 5, 6.

smoothly with increasing heating rates as shown in figure 39 (b). The behavior of peak V is rather different from other peaks. It always decreases with heating rate but the decrease is very sharp up to 13 Ks^{-1}. Past 13 Ks^{-1}, it decreases up to 17 Ks^{-1} and then drops to a very low value at heating rate higher than 19 Ks^{-1}. Figure 40 (a) and (b) shows the variation of activation energy of TLD-200 crystal with respect to heating rate (Ks^{-1}).
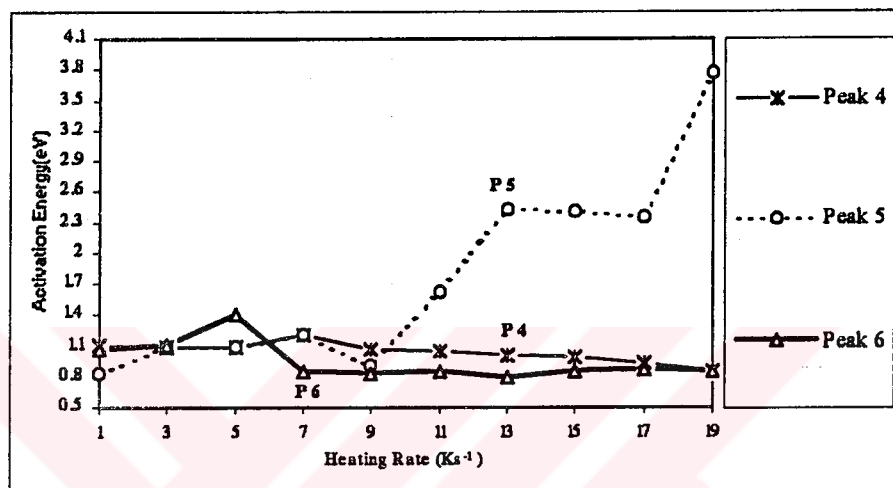
(b)
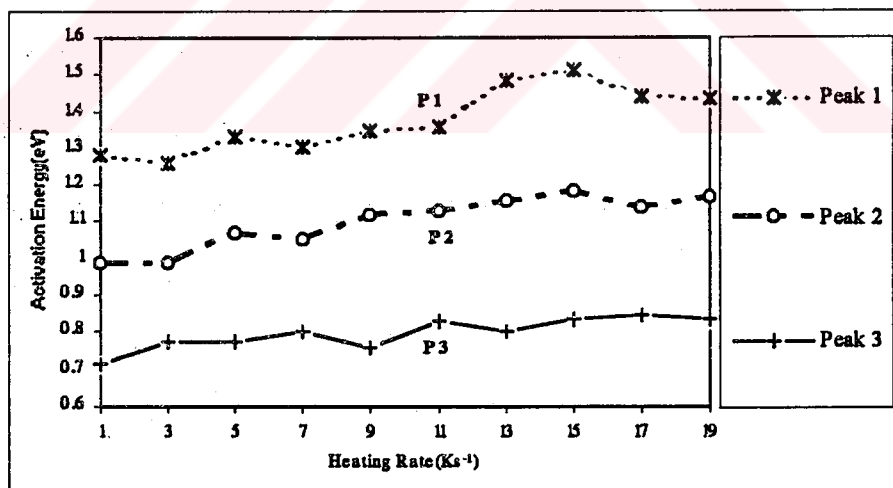
(a)

Figure 40 Variation of activation energy of TLD-200 crystal due to

heating rate (Ks^{-1}). **(a)** Peaks 1, 2, 3 and **(b)** Peaks 4, 5, 6.

In figure 40 (a) all peaks(1,2,3) have a smooth upward tendency with increasing heating rate, although some slight drops are observable for all three peaks at different heating rate. The changes in the activation energy of the peaks 4,5 and 6 are very different, especially in peak 5 as shown in figure 40 (b). The activation energy of peak IV is very slightly affected with heating rate. It always decreases very smoothly except that a small increase is observable at 7 Ks^{-1}. Very noticeable changes take place in the activation energy of peak V. It first slightly increases up to 7 Ks^{-1}, then drops to its lowest value at 9 Ks^{-1}, and then starts increasing again. Past 13 Ks^{-1}, it shows a very small decrease up to 17 Ks^{-1} and then sharply rises to its maximum value. Except a noticeable increase that occurs at the heating rate between 3 and 7 Ks^{-1}, the activation energy of peak VI is almost unaffected with increasing heating rate above 7 Ks^{-1}.

Figure 41 indicates the changes of maximum peak temperatures of TLD-200 crystal due to heating rate (Ks^{-1}). Generally, the maximum peak temperatures of all
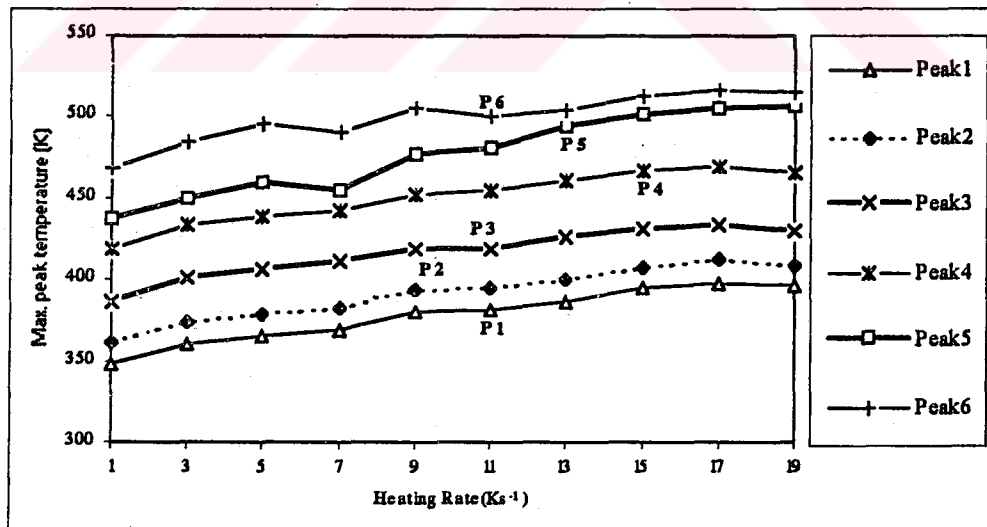

Figure 41 Variation of maximum peak temperatures of TLD-200 sample with respect to heating rate (Ks^{-1}).

the glow peaks of TLD-200 crystal are moved to the higher temperatures with increasing heating rate. This is of course to be expected, since previous studies about the effect of heating rate on different dosimetric crystals provided the similar results. As seen from figure 41, some slight drops in the maximum peak temperature are also observable. We think that they are probably due to the experimental errors.

The variation of FOM(figure-of-merit) due to heating rate is shown in figure 43. It is known that if the FOM values are between 0 and 2.5, then the fits made to the experimental values are accepted to be reasonably good. Since our values are in these limits, then we can say that we obtained good fits [22].
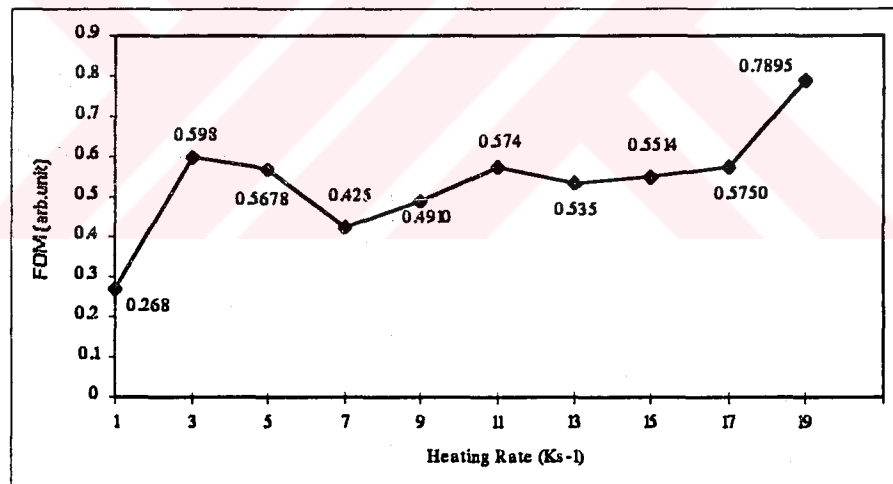

Figure 42 Variation of FOM derived from CGCD program due to the heating rate (Ks^{-1}) of TLD-200 crystal.

4.5 The effect of dose rate on glow curves of TLD-200 and its

kinetic parameters

In this part of the study, the sample exposed to the time dependent β-dose rate starting from 10 seconds until 1.5 hours has been investigated. The irradiation of procedure was done at the room temperature, which was about 293.15 ± 2 K. The sample was irradiated with ^{90}Sr-^{90}Y β-source at different time intervals to determine the effect of dose rate on the glow curve of TLD-200 sample and its kinetic parameters. The results are presented in figures 43-49.
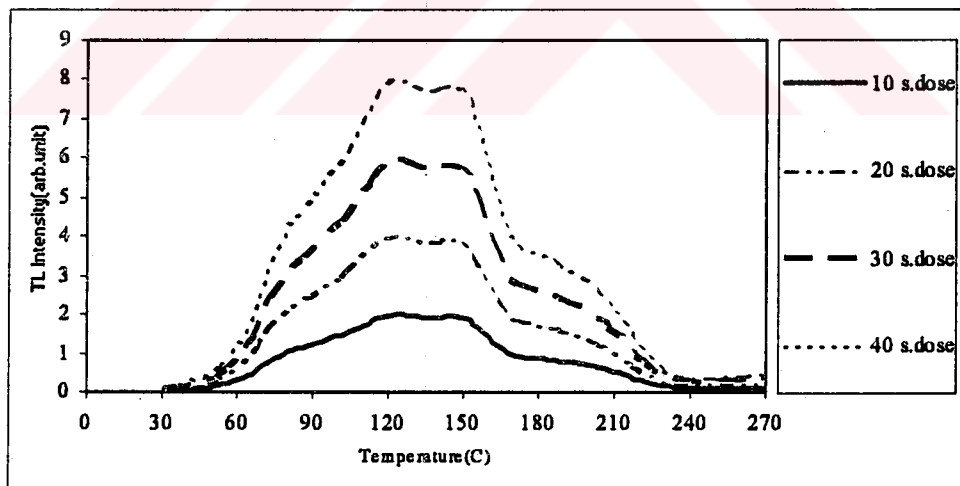

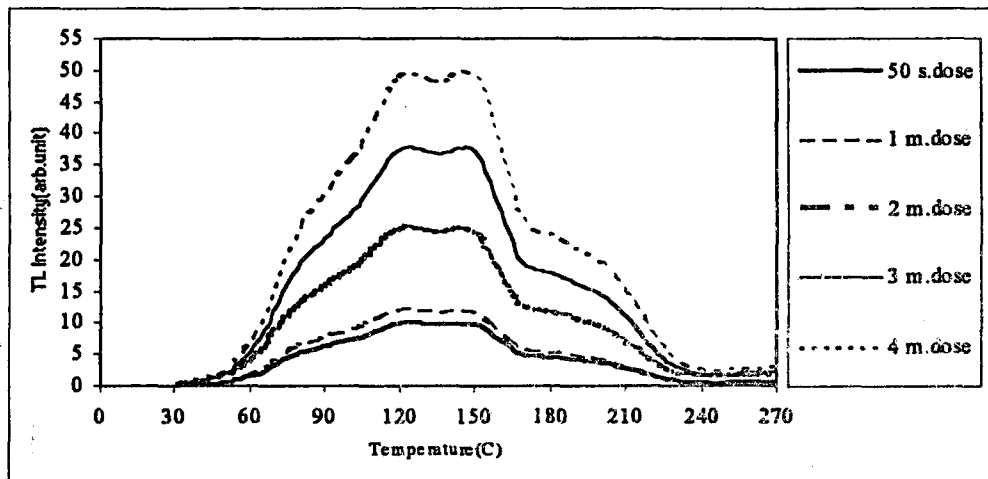**Figure 43**   TL Intensity of TLD-200 (CaF$_2$:Dy) crystal as a function of temperature for various dose rates.

Figure 44   TL Intensity of TLD-200 (CaF$_2$:Dy) crystal as a function of temperature
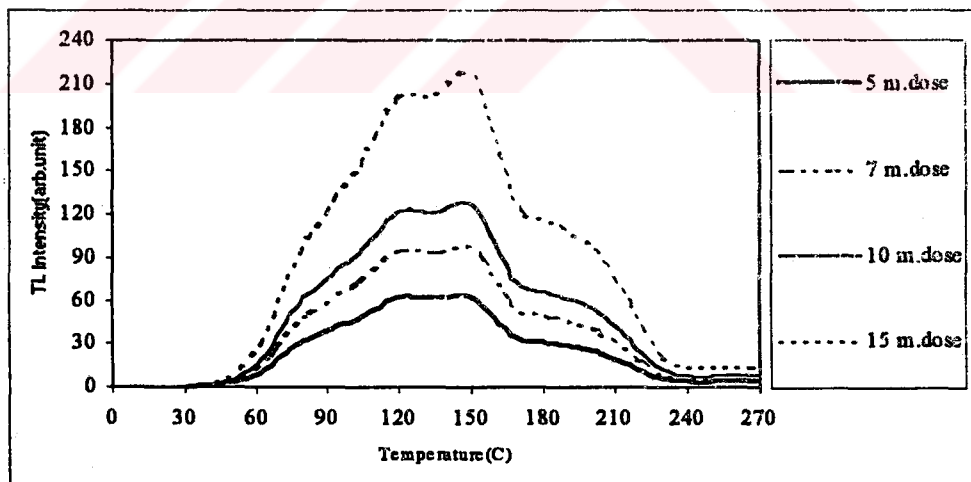
for various dose rates.

Figure 45   TL Intensity of TLD-200 (CaF$_2$:Dy) crystal as a function of temperature
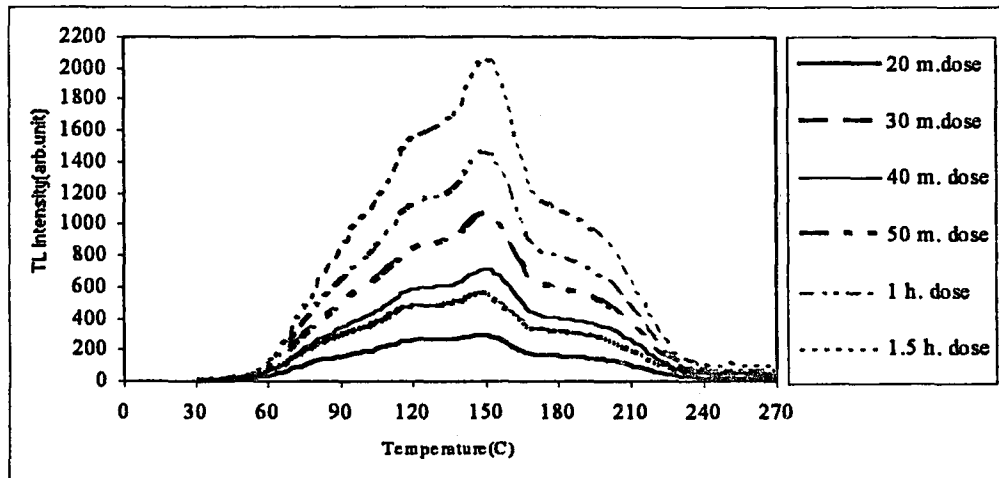
for various dose rates.

69

Figure 46 TL Intensity of TLD-200 (CaF$_2$:Dy) crystal as a function of temperature for various dose rates.

It is obviously seen from the above figures that total thermoluminescence intensity always increases with increasing dose rate. The reason is that as the dose rate increases more electrons are removed from the orbitals, as a result the number of electrons in the trap centers increases. Hence, during heating process more electrons make recombination in the recombination centers and emits lights. This results in a higher increase in the intensity of the glow peaks Another point to be motioned is that the maximum peak temperatures are found to be unchanged in all dose rate experiments.

Figure 47 shows the variation of peak areas of the glow peaks as a function of irradiation time.
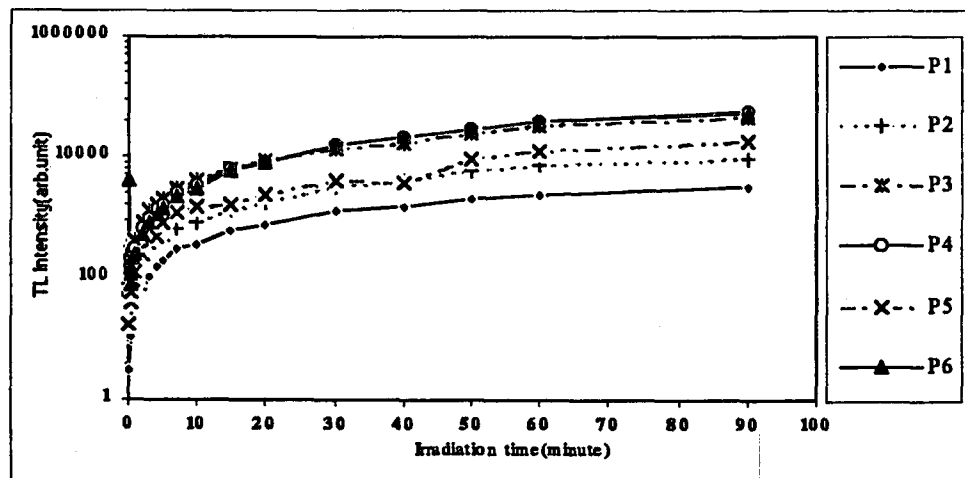

Figure 47 Variation of the value TL Intensity of peaks of TLD-200 crystal with respect to dose time.

70

It is obvious that peak areas of all the peaks always increases with increasing dose rate. The increase is exponential in the short irradiation time. Past 10 m, the TL intensity still increases in a very small step.

Figure 48 (a) and (b) shows the alteration of activation energy of glow peaks of TLD-200 as a function of irradiation time. The activation energy of peak III seems to be unaffected by the dose rate as shown in figure 48 (a). On the other hand peak I and peak II show an opposite behavior. While peak I drops sharply, peak II rises up quickly at low dose rates up to 10 minutes. Then the activation energy of both peaks level off at higher dose rates.

The change in the activation energy of peak V is quite remarkable as seen from figure 48 (b). At low dose rates, the activation energy of peak V indicates a zigzag behavior up to 7 m at which it drops to its minimum value. Past 7 m it increases sharply to a value 1.1 eV at 15 m and then drops again at 20 m A remarkable increase occurs from 20 to 40 m, at which it reaches to its maximum value 1.35 eV. Past 40 m, it shows a marked drop at 50 m and then levels off. Peak IV and VI also show up and down behavior at about 10 m Past 10 m peak VI continuos to make up and down pattern, while as peak IV shows slight decrease up to 50 m Then, like peak V the activation energy of peak IV and VI also level off above 50 m.
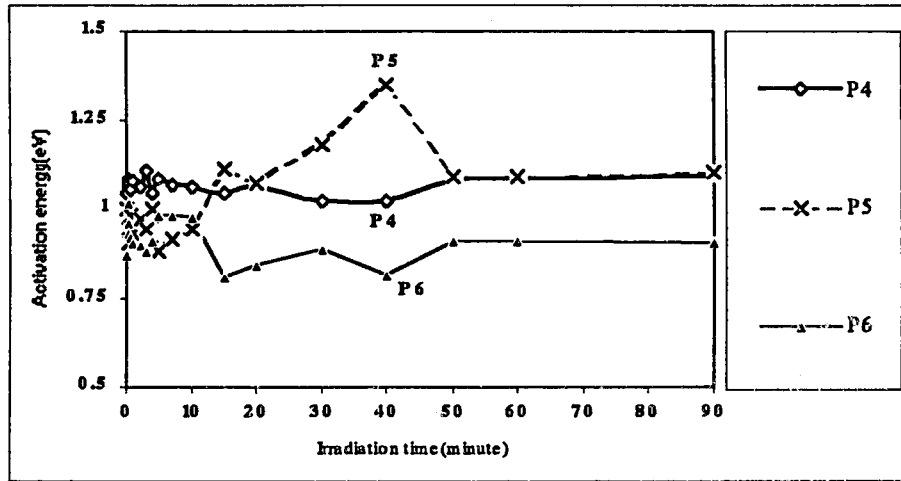
(b)
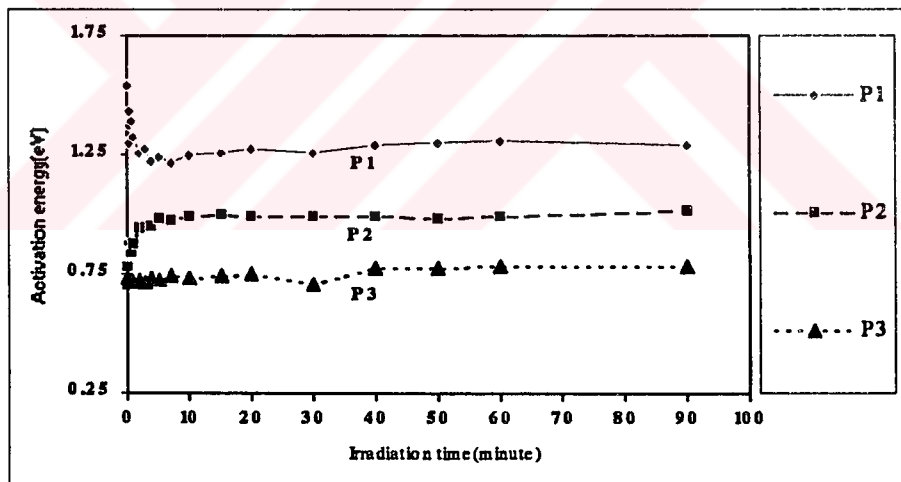
(a)

Figure 48   Variation of activation energy of peaks of TLD-200 crystal

with respect to dose time. **(a)** peaks 1, 2, 3 and

(b) peaks 4, 5 and 6.

Figure 49 constitutes the variation of FOM (arb. unit) with respect to irradiation time. FOM data clearly express that there is no doubt on goodness of fit. Since the values are between 0 and 2.5 [22].
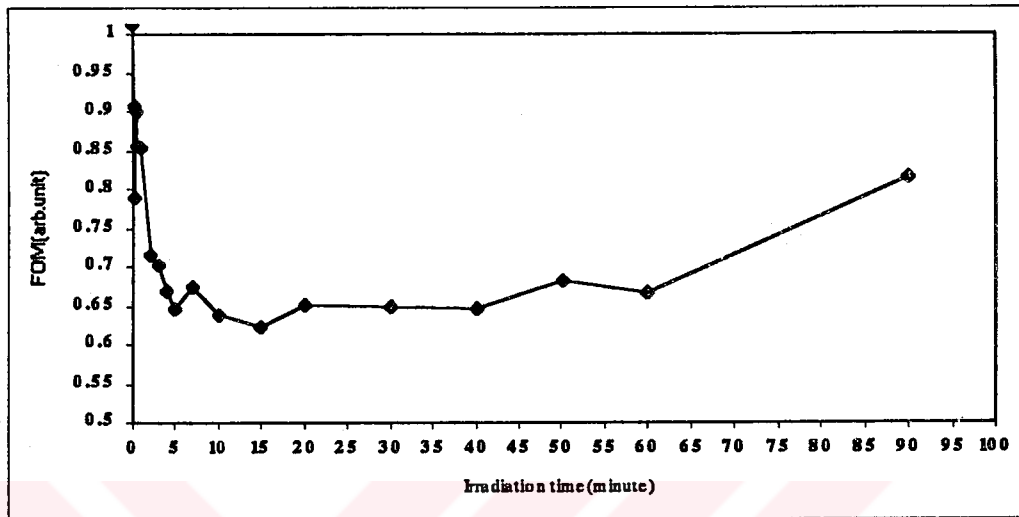

Figure 49   Variation of FOM for TLD-200 sample.

4.6 Fading of glow curves of TLD-200 (CaF₂:Dy) Crystal

Until here many properties of $CaF_2:Dy$ have been investigated. Finally, we have examined the fading characteristics of this crystal. In this process, we have used 5 samples having the same characteristics but different sizes. Samples irradiated to a suitable dose rate (5 minutes β-dose) have been put into box having no open side and left there for 1, 2, 3, 4, 5, 6, 7, 8, 9, 10, 11, 12, 13, 14, 15, 17, 18, 19, 20, 25, 30, 35, 40, 45, 50, 55 and 60 days. The inside temperature of the box was about 291.15 ± 4 K. The samples then were taken out from the box and immediately read out at a heating rate 1 Ks^{-1}. The results are analyzed by using CGCD computer programming and presented in figures 50-60.
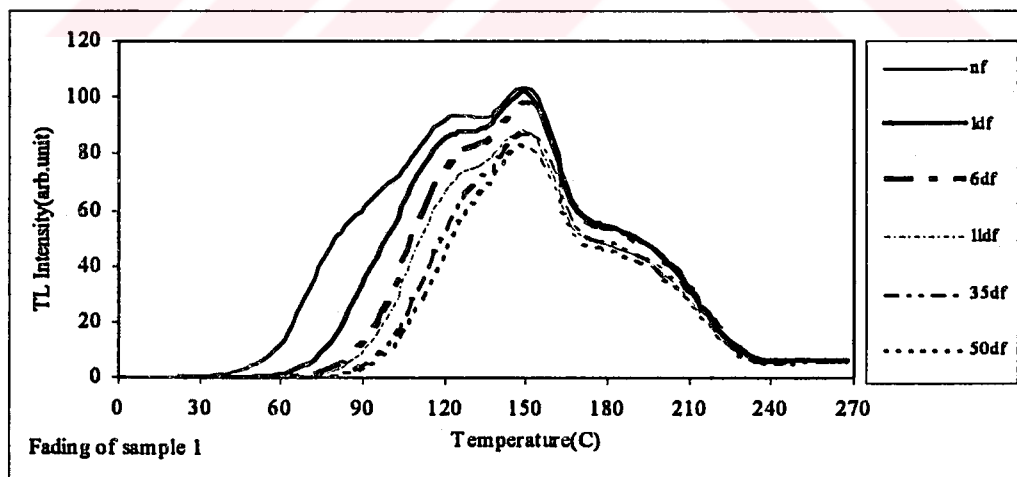

Figure 50 Fading of sample 1 (TLD-200 crystal) during 1, 6, 11, 35, and 50 days.
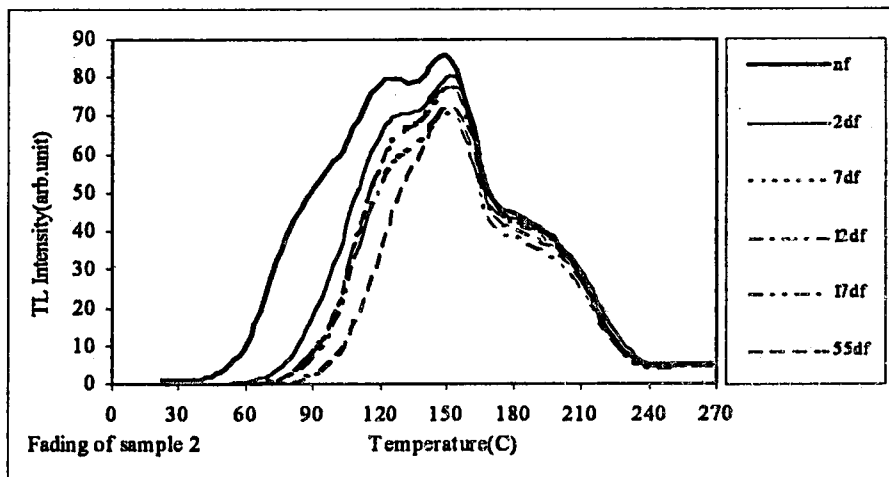
Figure 51 Fading of **sample 2** (TLD-200 crystal) during 2, 7,12, 17, and
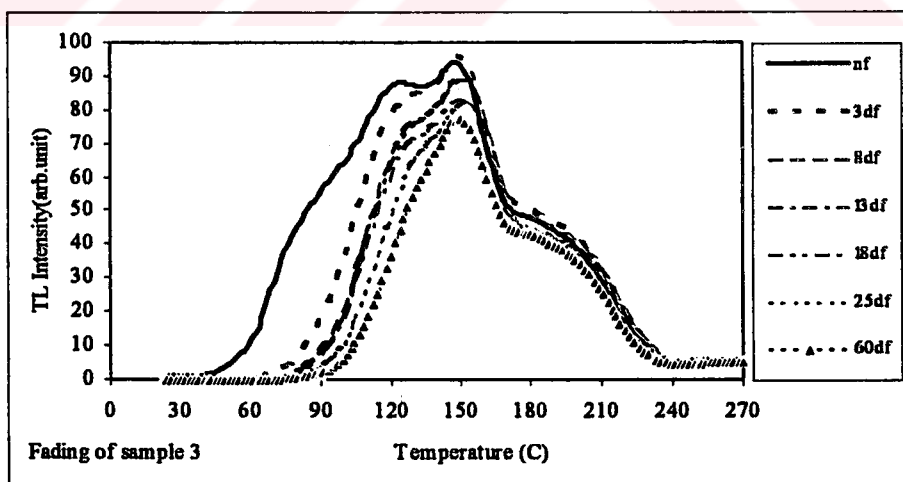
55 days.

Figure 52 Fading of **sample 3** (TLD-200 crystal) during 3, 8, 13, 18, 25,
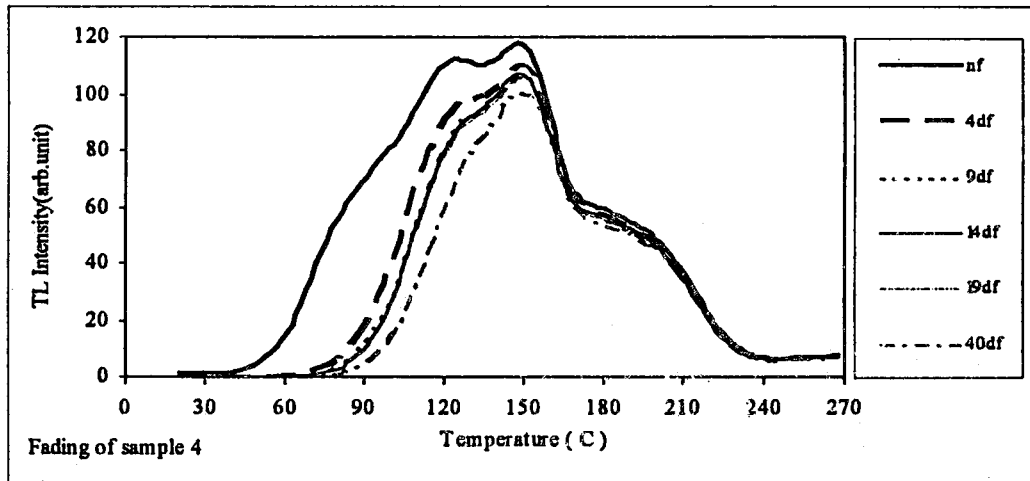
and 60 days.

Figure 53 Fading of sample 4 (TLD-200 crystal) during 4, 9, 14, 19, and

40 days.
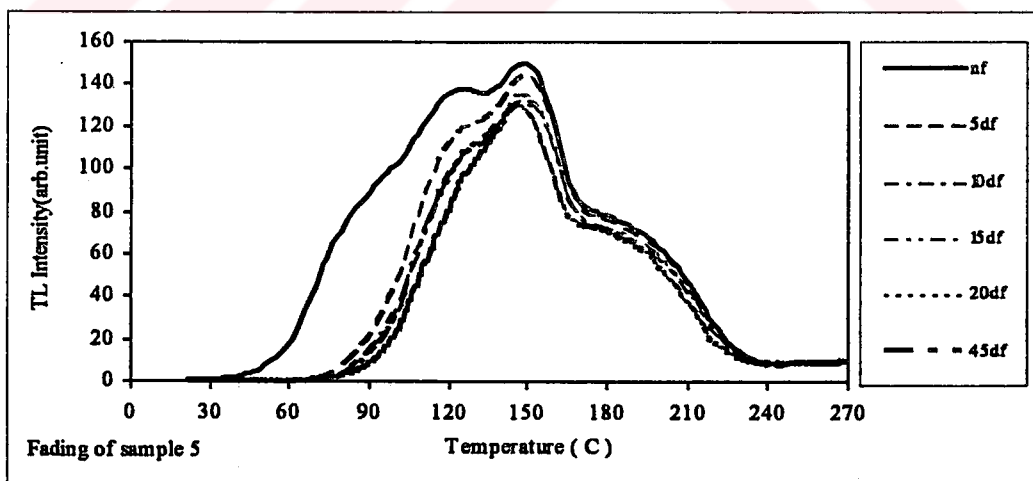
Figure 54 Fading of sample 5 (TLD-200 crystal) during 5, 10, 15, 20 and

45 days.

As seen from figures 50-54, all the samples fade away significantly. This means that fading is an important drawback in the utilization of CaF_2:Dy crystal in dosimetric applications.The main cause of fading is that during the waiting period, some of the shallow traps are empitied. Fading usually occurs in many dosimetric crystals, but the amount of fading determines the applicability of the crystals as dosimeter and their application areas as dosimetric materials. Nevertheless, fading is an undesired property and one of the disadvantages of the dosimetric materials.

Figures 55-59 show the variation of peak areas of samples 1-5 as a function of fading time (day).

Figure 55 Variation in TL peak areas of sample 1 (TLD-200 crystal) with respect to fading time (day).

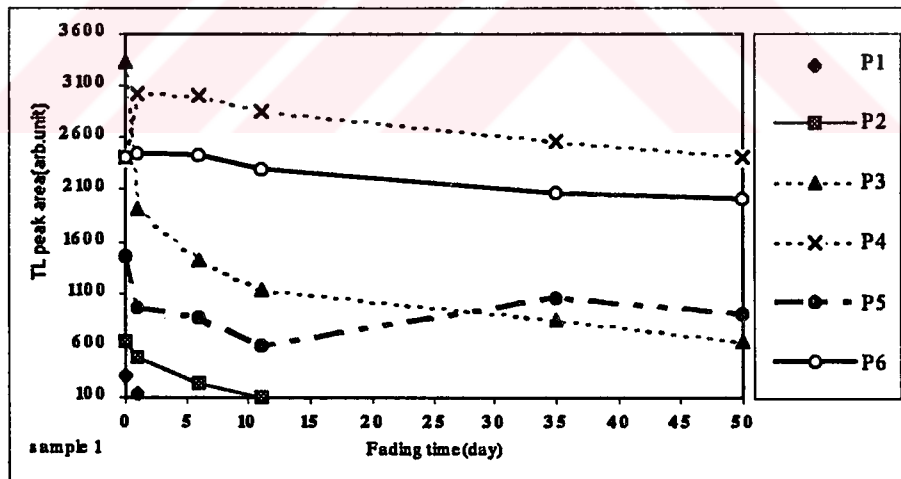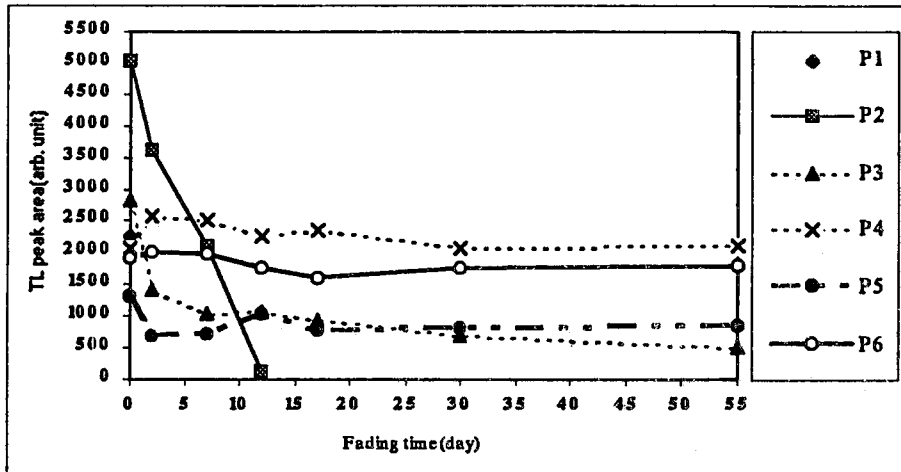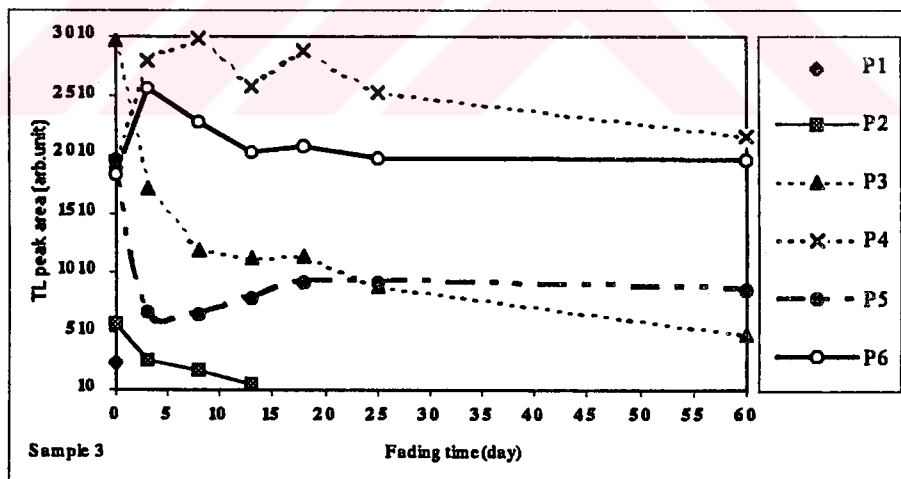**Figure 56** Variation in TL peak areas of sample 2 (TLD-200 crystal) with respect to fading time (day).

Figure 57 Variation in TL peak areas of sample 3 (TLD-200 crystal) with respect to fading time (day).
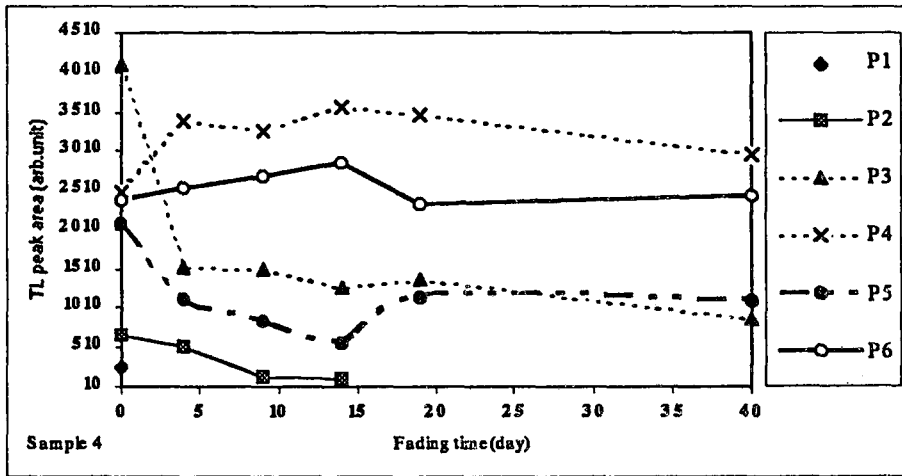
Figure 58 Variation in TL peak areas of **sample 4** (TLD-200 crystal) with respect to fading time (day).
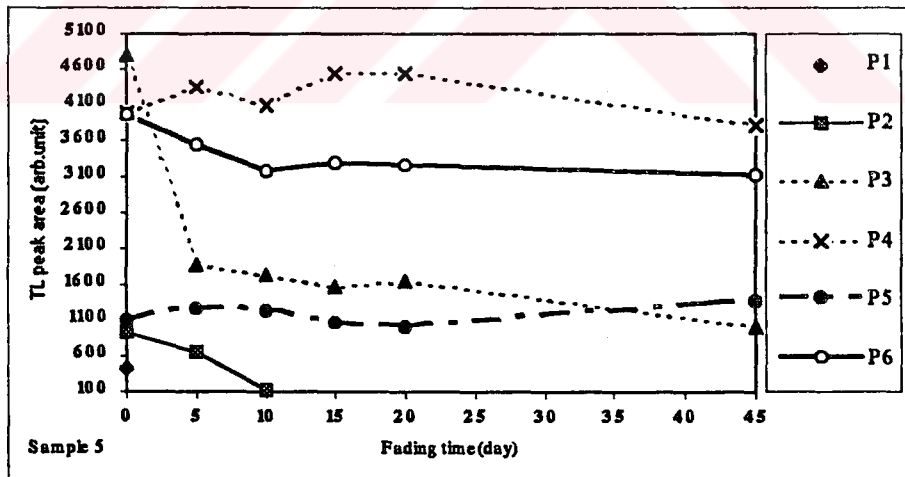
Figure 59 Variation in TL peak areas of **sample 5** (TLD-200 crystal) with respect to fading time (day).

Peak I fades away immediately after one or two days as seen from figures 55 through 59. Complete fading of peak II takes place in 10-15 day. Fading of peak III is very drastic in the first couple of days. Then it fades away very slowly. Peak IV, on the other hand, shows an opposite behavior. Its peak areas first dramatically increases in the first days of fading time and then seems to decrease very slowly. Fading of peak V is rather interesting. Its peak areas first significantly decreases within a few days and then shows a considerable increase with longer fading time. The behavior of peak VI is not as dramatic as that of other peaks. It first makes a small increase, then drops with increasing fading time, and then seems to level off with longer fading time.

The variation of the activation energy of samples 1-5 as a function of fading time (day) are illustrated in figures 60-64.
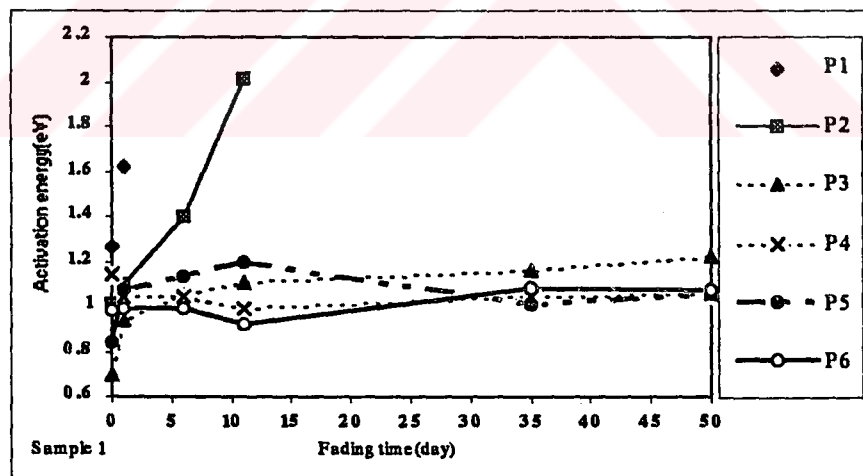
Figure 60 Variation of activation energy of **sample 1** (TLD-200 crystal) due to fading time (day).

80
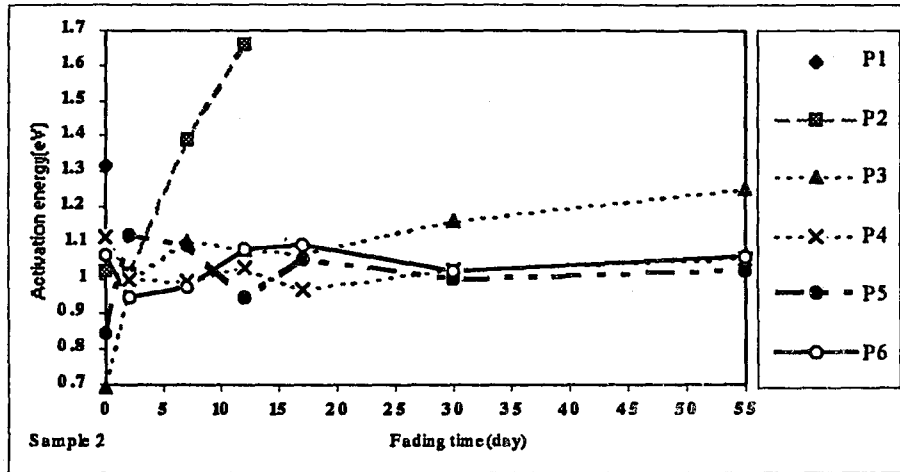
Figure 61 Variation of activation energy of sample 2 (TLD-200 crystal) due to
fading time(day).
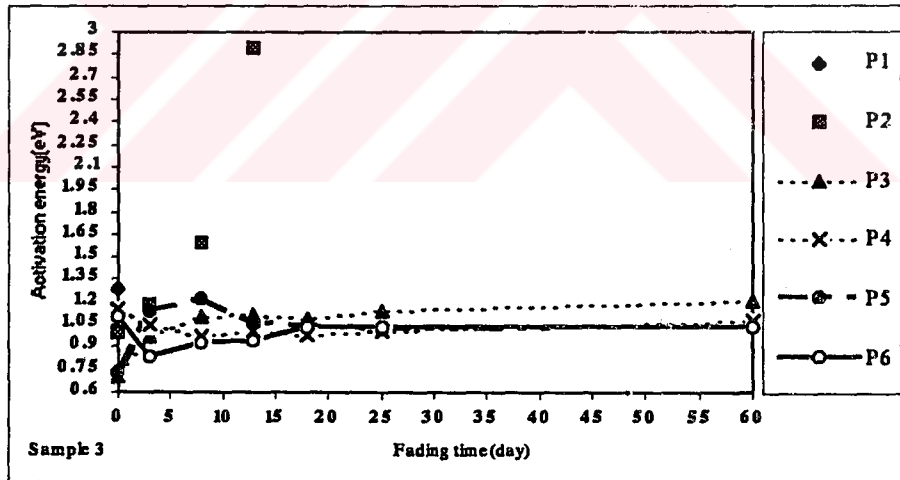
Figure 62 Variation of activation energy of **sample 3** (TLD-200 crystal) due to
fading time(day).
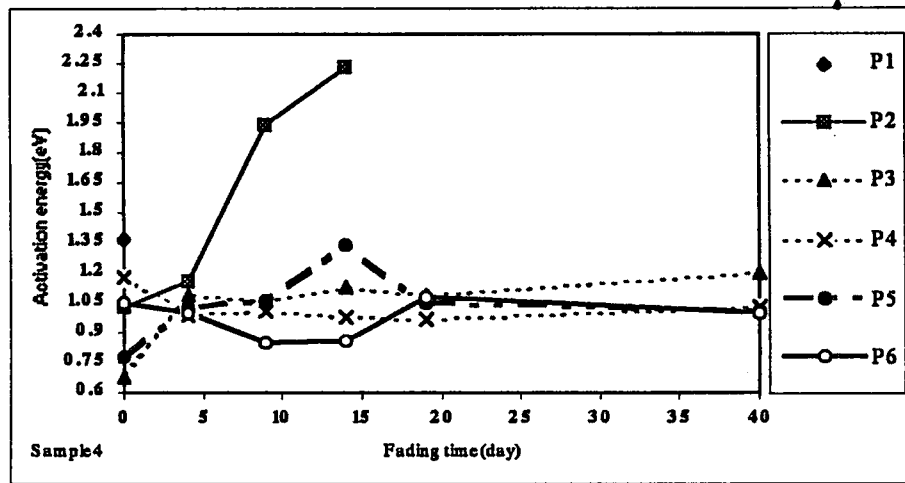
Figure 63 Variation of activation energy of **sample 4** (TLD-200 crystal) due to fading time(day).
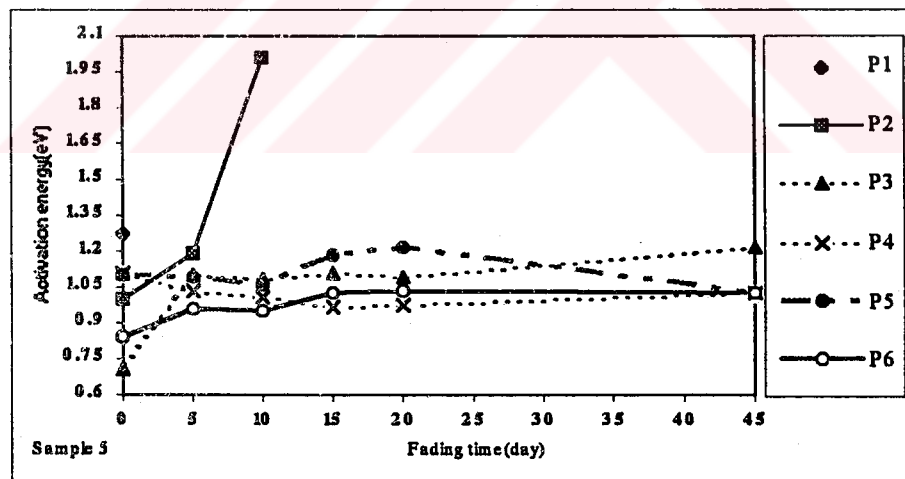
Figure 64 Variation of activation energy of **sample 5** (TLD-200 crystal) due to fading time(day).

Since peak I fades away immediately in the first two days, we have only one or two data for peak I in these figures. The activation energy of peaks I and II sharply increases with increasing fading time until they disappear. Activation energy of peak III always increases, but the increase in the first part of fading time is much more significant than the later time. Peak IV first considerably drops in the early part of fading time and then seems to level off with some small up or down changes. Opposite to the behavior of peak IV, peak V first makes a quick rise and then slowly decreases with some fluctuations as the fading time increases. The changes in the activation energy of peak VI is very interesting. It first decreases and increases considerably and then decreases again but slightly with fading time.

CHAPTER   5

CONCLUSION

Thermoluminescence dosimeters have found a wide range of application areas in scientific disciplines such as personnel monitoring, environmental dosimeters, health and medical physics and in another areas. Many crystals have been developed to fulfill the requirements for a good dosimeter, however, only eight materials are found to be suitable for applied radiation dosimeter. One of these crystals is the CaF_2 , which naturally exists in nature. This crystal is referred to TLD-200 when doped with Dy element. This TLD-200 dosimeter is found to have some desired properties and drawbacks. One of the most important advantage of this dosimeter is the very high intensity which is much higher about 15 times than that of TLD-100 (LiF:Mg,Ti) crystal. An other important properties of TLD-200 is its linear response to radiation

over a wide range of absorbed doses (up to 50 Gy). Fading is very high in this material due to the presence of the low temperature peaks, which is one of its main drawbacks. Compared to the literature on TLD-100 and some other dosimeters, relatively very few studies have been carried out on CaF_2:Dy crystals. It is found that no study has been done to determine the kinetic parameters of glow peaks CaF_2:Dy crystal. Therefore, the purpose of this work is defined as to investigate the thermoluminescence properties and to determine the effect of post-annealing, heating rate, dose rate and fading on kinetic parameters of CaF_2:Dy crystals.

In the analyses of the glow curves of TLD-200, several techniques were utilized such as curve deconvolution, peak shape, isothermal decay, and initial rise method. The first and general order kinetic formulas are applied with a computerized deconvolution technique(CGCD) to CaF_2:Dy glow curves. The CGCD analysis have shown that CaF_2:Dy glow curves consists of six peaks in the temperature range of 0 ^{0}C and 270 ^{0}C. However, some studies report 4 or 5 peaks for CaF_2:Dy crystal. This difference is due to the high rate of fading of peak 1, which dies out in one day. Hence, if the TL reading of the sample is made one day after the irradiation, first peak will not appear in the glow curves of CaF_2:Dy dosimeter. Some other factors such as the type of irradiation source, heating rate, and dose rate also affect the glow curves.

The CGCD analysis have also shown that all the peak except peak VI have a first order kinetic. Combined results of isothermal decay and peak shape method have prevailed that the kinetic order of peak VI is between 1.55 and 1.6.

The results of post-irradiation annealing , heating rate, dose rate and fading have indicated that all these processes have great influences on the glow curves and kinetic parameters of CaF_2:Dy crystal. This means that the trap centers interact with

each other during these processes. The possible explanation of thermoluminescence and defect interactions in CaF_2:Dy during these processes can be made as follows:

β-ray irradiation reduces trivalent Dy^{+3} ions to the divalent state and at the same time produces hole centers, which become mobile at high temperatures. If such a hole moves to the proximity of a divalent Dy^{+2} ion, it may recombine with an electron, leaving the ion in a excited trivalent state. As a result, the decay of Dy^{+3} ion to the ground state is observed as thermoluminescence. Merz and Pershan (1967) have suggested that below room temperature most of the Dy^{+3} ions involved in the TL process are those in cubic sites[49]. The reduction of many Dy^{+3} ions in cubic sites to the Dy^{+2} state has been reported at and below room temperature (Hayes and Steable, 1974 [50].; Royce *et al.*, 1984 [51]). For RE^{+3} ions (Dy^{+3}, Tm^{+3} and Sm^{+3}) in sites with symmetry less than cubic giving TL about room temperature it is suggested that hole traps consisting of fluorine aggregates break up, resulting in interstitial fluorine atoms diffusing to divalent RE^{+2} ions and converting then into RE^{+2}-F_i (Hayes and Staebler 1974; Merz and Pershan, 1967). However, it is also possible that the TL emission at low temperature may originate from ions in sites having other than cubic symmetry, and at high temperature from cubic sites, because the compensators become mobile and leave RE^{+3} ion in a cubic environment (Schlesinger and Whippy, 1969)[52]. For CaF_2:Dy it is though that the TL emission originates from a mixture of cubic and other the lower symmetry sites (Schlesinger and Kwan, 1971)[53]. Although the knowledge of defect centers formed as a result of RE doping is considerable, there is still controversy regarding the concentration and temperature dependency of the relative abundance of different impurity and defect centers.

It has been observed that the peak areas and activation energy of all the peaks of CaF_2:Dy samples are greatly changed as a result of post-annealing treatment, irradiation dose, heating rate, and fading. In all experiments identical CaF_2:Dy samples were used, however, during the fading experiments five samples with different sizes were used. The use of five different samples made the analyses of the fading results more difficult than it should be. Therefore, we suggest that in further studies one should use the identical samples and expose them to the identical fading conditions. The value of the activation energy of glow peak VI determined by three different method was in very good agreement as given in Table 4.

In conclusion, this work has provided a detailed information about the thermoluminescence characteristic and kinetic parameters of CaF_2:Dy crystal.

LIST OF REFERENCES

[1]- Daniels F., Boyd C.A. and Sounders D.F., 1953. "Thermoluminescence as research tool", *Science*, 117, pp. 343.

[2]- Cameron J.R., Suntharalinga N. and Kenney G.N., 1968. Thermoluminescent Dosimetry, *University of Wisconsin Press*, Madison.

[3]- Bacci C., Draghi V., Furetta C. and Rispoli B., 1989. "Fading in CaF_2 Tm/Dy TL Phosphors used in environmental radiation monitoring", *IEEE Transactions on nuclear Science*, 36,1, pp. 1154-1156.

[4]- Jain V. K.,1990. "Charge carrier trapping and thermoluminescence in calcium fluoride based phosphors", *Radiat. Appl. Instrum. Part C.*, 36, 1, pp. 47-57.

[5]- Azorin J., Furetta C. and Gutiérrez A., 1989. " Evaluation of the kinetic parameters of CaF_2:Tm TLD-300 thermoluminescence dosimeters", *J. Phys. D:Appl. Phys.*, 22, pp. 458-464.

[6]- Becker K., 1973. 'Solid state dosimetry", *CRC Press*, pp. 65-66.

[7]- Horowitz Y.S. , 1984. Thermoluminescence and Thermoluminescent Dosimetry I-III, *CRC Press*, Boca Raton, Florida.

[8]-McKeever S.W.S.,1985. 'Thermoluminescence of Solids", *Cambridge University Press*, pp. 64-66.

[9]- Arkhangel'skaya V.A., 1964. *Opt. Spectrosc.*, 16, pp.343.

[10]- Merz J. L. and Pershan P. S., 1967. *Phys. Rev.*, 162, pp. 217-235.

88

[11]- Sunta C.M., 1984. *Radiat. Protect. Dosim.*, **8**, pp.25.

[12]- Driscoll C.M.H., Barthe J.R., Oberhofer M., Busuoli G. and Hickman C., 1986. *Radiat. Protect. Dosim.*, **14**, pp.17.

[13]- Furetta C. and Lee Y.K., 1983. *Radiat. Protect. Dosim.*, **5**, pp.57.

[14]- Alonso P.J. and Alcal R., 1980. *J. Luminescence*, **21**, pp. 147.

[15]- Jain V. K. and Jahan M.S., 1985a. *Phys. Stat. Sol. a*, **92**, pp.237.

[16]- Jain V. K. and Jahan M.S., 1985b. *J. Phys. D: Appl. Phys.*, **18**, pp.L15.

[17]- Jain V. K. and Jahan M.S., 1985c. *Bull. Am. Phys. Soc.*, **30**, pp.1783.

[18]- Pradhan A.S. and Rassow J., 1987. *Nucl. Instrum.Methods*, **A255**, pp.234.

[19]- Driscoll C.M.H., Francis T.M. and Richards D.J., 1984. *Radiat. Protect. Dosim.*, **9**, pp.269.

[20]-Fillard J.P., Gasiot J.,Sanz L.F. and De Sala J.A., 1977. *J. Electrostat.*, **3**, 133.

[21]- Fillard J.P., Gasiot J. and Manifacier J.C., 1978. *Phys. Rev.*, **B18**, pp.4497.

[22]- Gasiot J. and Fillard J.P., 1977. *J. Appl. Phys.*, **48**, pp. 3171.

[23]- Kelly P.J., Laubitz M.J. and Brounlich P., 1971. *Phys. Rev.*, **B4**, pp.1960.

[24]- Shenker D. and Chen R., 1972. *J. Compt. Phys.*, **10**, pp.272.

[25]- Hagebeuk H.J.L. and Kivits P., 1976. *Physica*, **83B**, pp.289.

[26]- Kivits P. and Hagebeuk H.J.L., 1977. *J. Luminesc.*, **15**, pp.1.

[27]- Kivits P., 1978. *J. Luminesc.*, **16**, pp.119.

[28]- Chen R., McKeever S.W.S and Durrani S.A.,1981. *Phys. Rev. B*, **24**, pp.4931.

[29]- Adirovitch E.I., 1956. *J.Phys.Rad.*, **17**, pp. 705.

[30]- Haering R.R. and Adams E.N., 1960. *Phys.Rev.*, **117**, pp. 451.

[31]- Halperin A. and Braner A.A., 1960. 'Evaluation of Thermal Activation Energies from Glow Curves", *Phys.Rev.*, **117**,pp. 405-415.

[32]- Bull R.K., McKeever S.W.S., Chen R., Mathur V.K., Rhodes J.F. and Brown M.D., 1986. 'Thermoluminescence kinetics for multipeak glow curves produced by the release of electrons and holes", *J.Phys.D:Appl.Phys.*, **19**, pp.1321-1334.

[33]- Dharamsi A.N. and Joshi R.P., 1991. "An approximate rate equation analysis for bleaching and excitation of thermoluminescence", *J.Phys.D:Appl. Phys.*, **24**, pp.982-987.

[34]- Sakurai T., 1995. 'New method for numerical analysis of thermoluminescence glow curves", *J.Phys.D:Appl.Phys.*, **28**, pp.2139-2143.

[35]- May C.E. and Partridge J.A., 1964. 'Thermoluminescent kinetics of alpha irradiated alkali halides", *J.Chem.Phys.*, **40**, pp. 1401-1409.

[36]- Garlick G.F.J. and Gibson A.F., 1948. 'The electron trap mechanism of luminescence in sulphide and silicate phospors", *Proc.Phys.Soc.*,**60**, pp.574-590.

[37]- Grossweiner L.I., 1953. "A note on the analysis of first-order glow curves", *Journal of Applied Physics*, **24**, pp- 1306-1307.

[38]- Lushchik C.B., 1956. "The investigation of trapping centers in crystals by the method of thermal bleaching", *Sov.Phys. JEPT*, **3**, pp- 390-395.

[39]- Halperin A. and Braner A.A., 1960. "Evaluation of Thermal Activation Energies from Glow Curves", *Phys.Rev.*, **117**,pp. 405-415.

[40]- Chen R., 1969. "On the Calculation of the Activation Energies and Frequency Factors from Glow-Curves", *Journal of applied Physics*. **Vol.40**, pp.570.

[41]- Podgorsak E.B., Moran P.R. and Cameron J.R., 1971. "Interpretation of resolved glow curve shapes in LiFTLD-100 from 100 to 500 K", *Proc. 3rd Int. Conf. on Luminesc. Dosim.*, Ris Rep., **249**, pp. 1-7.

[42]- Horowitz Y. S., Moscovitch M., 1986. "Computerized glow curve deconvolution applied to high dose 1-10 Gy TL Dosimetry", *Nucl. Instrum. Methods Phys. Res. A*, **243**, pp. 207-214.

[43]- Horowitz Y. S., Moscovitch M., 1986. "Computerized glow curve deconvolution applied to ultralow dose LiF TL Dosimeter", *Nucl. Instrum. Methods Phys. Res. A*, **244**, pp. 556-564.

[44]- Balian H. G. and Nelson W. E., 1977. "Figure fo Merit FOM;an improved criterion over the normalized chi-squared test for assessing goodness-of-fit of Gamma-ray spectral peaks", *Nuclear Inst. and Methods*, **145**, pp. 389-395.

[45]- Sushil K. M. and Nelson W. E., 1979."IFOM, A formula for universal assestment of goodness-of-fit of Gamma-ray spectra", *Nuclear Inst. and Methods*, **166**, pp. 537-540

[46]- *Model 3500 Manual TLD Reader User's Manual*, July 30 1994. Publication No 3500-0-U-0793-005.

[47]- *9010 Optical Dating System User Manual*, Dec. 1993.

[48]- Chen R., 1984 . "Kinetics of thermoluminescence glow peaks", *Thermoluminescence and thermoluminescent dosimetry Edited Y. S. Horowitz*, Chap.3, pp. 49-88.

[49]- Merz J. L. and Pershan P. S., 1967. *Phys. Rev.*, **162**, pp. 217-235.

[50]- Hayes W. and Staebler D. L., 1974. In *Crystals with the Flourite Structure, Clarendon Press*, Oxford, pp. 415.

[51]- Royce G. A. *et al.*, 1984. *J. Luminescence*, **29**, pp. 205.

[52]- Schlesinger M. and Whippy P. W., 1969. *Phy. Rev.*, **177**, pp. 563.

[53]- Schlesinger M. and Kwan C. T., 1971. *Phy. Rev.*, **B3**, pp. 2852